VOL. 15 No. 11, pp. 297-324 MAY 1954

Philips Technical Review

DEALING WITH TECHNICAL PROBLEMS
RELATING TO THE PRODUCTS, PROCESSES AND INVESTIGATIONS OF
THE PHILIPS INDUSTRIES

EDITED BY THE RESEARCH LABORATORY OF N.V. PHILIPS' GLOEILAMPENFABRIEKEN, EINDHOVEN, NETHERLANDS

A LINE CONVERTER FOR THE INTERNATIONAL EXCHANGE OF TELEVISION PROGRAMMES

by J. HAANTJES and Th. G. SCHUT.

621.397.2

*The international relay of the London television broadcasts on the occasion of the Coronation was a spectacular proof of the possibility of converting television pictures of one scanning frequency into another. On a smaller scale, this had already been demonstrated a year previously, when broadcasts from Paris were relayed to England *). This article gives a description of the "line converter", which in June 1953 enabled the Dutch and West-German TV transmitters to relay programmes from London and Paris by effecting the necessary conversions from pictures of 405 and 819 lines respectively into 625 lines.*

At present, several different television standards are in regular use in Western Europe. They all have the same frame frequency, viz. 25 complete pictures per second (two interlaced frames forming one complete picture), but one of the points in which they differ is the number of lines per frame. An exchange of TV programmes among the West-European countries is therefore possible only if there are means available for converting pictures of one number of lines into those of another. This problem became urgent when, in France, the Netherlands and Western-Germany, the wish was expressed for relay-broadcasts of the B.B.C. transmissions scheduled for the Coronation. As is well known, such a relay network was indeed established [1]) and in general very satisfactory pictures were received. The 405-line signal was relayed, via a chain of link transmitters, to Paris, where the Radiodiffusion-Télévision Française took care of its conversion into an 819-line signal [2]). A second chain of link transmitters took the 405-line signal from Cassel (Northern France) to Breda (Holland), where it was converted into a 625-line signal. Two link transmitters set up in Breda relayed this converted signal to the Dutch TV stations at Lopik and Eindhoven. Two further link transmitters beamed the signal from Eindhoven to an existing network of similar transmitters in Germany.

In this article we shall first consider some general aspects of the problem of line conversion, and then give a more detailed account of the system used in Breda.

General aspects of the problem

Indirect method

One of the ways of showing TV pictures to a large audience, e.g. in a cinema, is the following. A film is made of the image on a picture tube; the film is developed, fixed, rinsed and dried at great speed, and immediately afterwards projected for the audience. It has been possible to reduce the time required for processing the film to 1-2 minutes.

Clearly, instead of being projected, the film can be run off through a film scanner, which is the usual procedure if films are to be broadcast by television. By virtue of the intermediate image on the film, the outgoing signal is no longer dependent on the

*) TV from Paris, Wireless World 48, 298-300, Aug. 1952.
[1]) Philips tech. Rev. 14, 358-360, 1953 (No. 12).
[2]) The link Paris-Lille in the map accompanying the article referred to in [1]) brings the 819-line signal from Paris to the transmitter at Lille. The transmitter in Berlin (not shown on the map) was also included in the West-German network.

number of lines of the original picture. This is called the *intermediate film process* — an *indirect* method, as opposed to the *direct* methods to be dealt with later.

This process has certain drawbacks. First of all, the photographing of TV pictures (50 frames per second) with a film speed of 25 frames per second is no easy matter; the obvious solution of moving the film during the frame blanking of the TV picture is not feasible with ordinary film cameras, as the time required for the film to move one frame is too long. In the second place, a highly elaborate installation is necessary for the rapid processing of the exposed film. Added to this are the costs of the film material. A further complication, also involving delay, is the fact that the sound has to be recorded as well. All this tends to make the intermediate-film method rather unattractive.

Direct methods

There are also methods which are practically delay-free and can, therefore, be considered as direct methods.

It is possible, for example, to reproduce the original TV picture in the form of a potential pattern on a flat plate (target plate), and then scan this pattern with an electron beam in accordance with the required number of lines. The formation of the potential pattern can be realized in two ways:

1) directly, by means of an electron beam modulated with the original signal, or

2) with the aid of an intermediate optical image, displayed on a picture tube, and viewed by a television camera (in this case the target of the pick-up tube of the camera is the plate on which the potential pattern is formed).

In the former case a special tube is required, containing a target plate, a "writing" and a scanning electron beam. (Alternatively, two tubes may be used — each with a target and one beam; whilst projection is taking place in one tube, the other is scanning; after one complete picture their functions are reversed, etc.) With this first method it has been found rather difficult to retain the original gradation of the picture.

It has been suggested that the second method has the drawback that, apart from the "electrical intermediate image" (the potential pattern), an optical intermediate picture is also required, and that each increase of the number of intermediate pictures will inevitably impair the image quality. This apparently reasonable argument, however, should not carry undue weight, for the following reasons. The intermediate optical picture can be directly watched and checked; also a large experience has been accumulated in the presentation of TV pictures on cathode-ray tubes and the prevention of possible faults — which cannot yet be said of the first-mentioned method.

It has further been suggested that in the method using an intermediate optical picture, it is not desirable to use a camera tube in which the secondary electrons can return to the target [3]); the resulting redistribution effect would cause the formation of spurious signals or "edge flare" to a disturbing degree. Camera tubes in which this redistribution effect occurs, are the iconoscope and the image iconoscope [4]). We know, however, that the image iconoscope — to mention only this

[3]) A. Cazalas, Problème de la transformation des standards de télévision, Onde électr. **31**, 178-183, 1951; V. K. Zworykin and E. G. Ramberg, Standards conversion of TV signals, Electronics **25**, 86-91, January 1952.

[4]) For the working principle of these tubes, see P. Schagen, H. Bruining and J. C. Francken, Philips tech. Rev. **13**, 119-133, 1951.

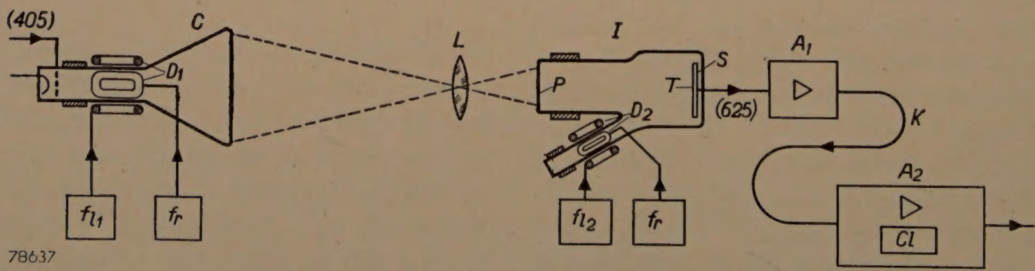

Fig. 1. Line converter with intermediate optical picture for converting a 405-line television picture into one of 625 lines. The 405-line picture is made visible in the conventional way on the screen of a (special) picture tube C (with deflection coils D_1; line frequency $f_{l_1} = 405 \times 25 = 10\ 125$ c/s, frame frequency $f_r = 50$ c/s). A lens L projects the image of C on the photo-cathode P of a camera tube (image iconoscope I). Its target (T) is scanned in accordance with the 625-line system (deflection coils D_2; line frequency $f_{l_2} = 625 \times 25 = 15\ 625$ c/s, frame frequency $f_r = 50$ c/s). S signal plate. A_1 pre-amplifier, K cable. A_2 main amplifier (with clamping circuit Cl, see further in this article).

tube — does not give rise to spurious signals if only the photo-cathode is sufficiently illuminated, although then the redistribution effect is rather strong. Without undue trouble, the light spot of the picture tube can be given a luminance sufficient for the image iconoscope to operate under favourable conditions.

This consideration, added to the fact that the image iconoscope is capable of producing images of excellent definition and gradation, led to the decision to use an image converter based on the system of an intermediate optical picture and an image iconoscope camera (*fig. 1*).

Before giving a further description of the equipment, we will deal with some disturbing effects which may occur, and the manner in which these have been counteracted.

Disturbing effects and their prevention

The following three disturbing effects are encountered with a line converter employing an intermediate optical image:

1) Superimposed on the photo-current of the camera tube is a signal corresponding to the original number of lines; without counter-measures, this signal would occur as a disturbing component in the output signal.

2) Interference will occur between the two numbers of lines.

3) Although the same picture-repetition rate is used over the whole of Western Europe (25 complete pictures per second), slight differences do occur, which give rise to beat effects.

These three effects will now be dealt with successively. Unless stated otherwise, we shall only consider conversion from 405 to 625 picture lines.

Presence of the original signal in the photo-current

The image on the picture tube of the line converter is not a "continuous" image, but a picture which is traced line by line by a moving light-spot. A corresponding light-spot therefore moves across the photo-cathode of the image-iconoscope. For the sake of convenience, we shall first assume that the picture to be transmitted is a surface of uniform brightness. The light-spot then has a constant brightness and thus gives rise to a constant photo-current, irrespective of position. At the end of each line, however, and also upon the completion of a frame, the light-spot disappears for a moment (due to the line blanking and frame blanking, respectively), and consequently the photo-current momentarily drops to zero.

The photo-current therefore contains Fourier components with the line frequency ($405 \times 25 = 10\,125$ c/s), with the frame frequency (50 c/s) and with multiples of the two. If an actual image is transmitted, then the light-spot varies in brightness and the photo-current will also contain Fourier components corresponding to the content of the image. Thus the character of the 405-line picture is still present to a considerable degree in the photo-current.

The photo-electrons impinge on the target, where they cause potential fluctuations, which are capacitively transferred to the signal plate. Hence the output signal of the image iconoscope consists of a mixture of 625-line and 405-line signals. To contend with this situation, two remedies have been resorted to, one being directed against the high frequency components, and the other against the low frequency components of the disturbing signal. Used in conjunction, these were found to deal effectively with the disturbance caused by the fluctuating photo-current.

High frequencies: Fluctuations of the photo-current can be reduced by using a long persistence phosphor for the picture tube of the line converter. The afterglow of the moving light-spot then smooths out the variations of the total photo-current, in particular those caused by the line and frame blanking signals.

The duration of the afterglow is limited by the fact that excessive afterglow would cause an objectionable blurring of movement, visible as blurs or smudges behind moving parts of the picture. It was found possible, however, to lengthen the afterglow to such an extent that at least the high-frequency components were smoothed out of the photo-current without creating objectionable blurring.

Willemite was chosen as the phosphor; it has an afterglow of approximately 13 milliseconds. After $^1/_{50}$ second, 20-25% of the original luminance remains, and after $^1/_{25}$ second still 5-6%. Willemite has a good fluorescent efficiency and the spectrum of the fluorescent light is favourable with respect to the spectral sensitivity of the photo-cathode. The colour of the light is green.

Low frequencies: The photo-current, and hence the output signal, still contain the low-frequency Fourier components of the original signal. These can be removed if the required signal contains a certain periodically recurring reference level, having a repetition frequency which is high compared to the disturbing frequencies. Due to the low-frequency disturbing components, this reference

level gradually varies, but by means of a suitable circuit, it can be restored to a fixed level. This is done in the manner illustrated in *fig. 2*.

In our particular case, the black level is used as the reference level. Since the image iconoscope does not transmit any "direct voltage", this level is not automatically present, but has to be specially introduced. An opaque strip is placed at one side of the picture on the photo-cathode. The part of the target corresponding to this strip lies at the side where the line-scanning begins and is scanned by the beam just before the beginning of each line. In this manner the black level is established, at the repetition frequency of the scanning lines.

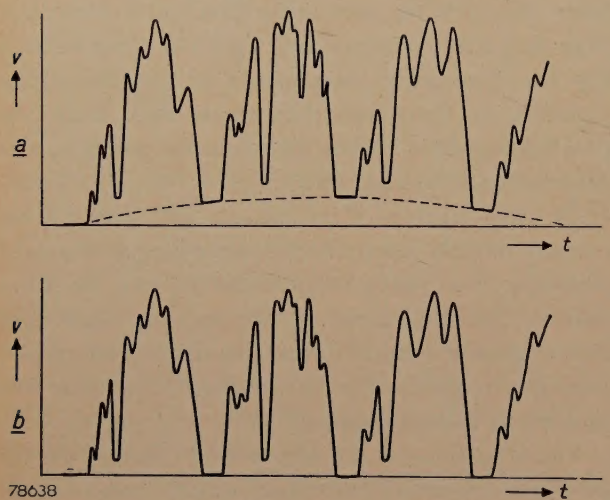

Fig. 2. Output signal v (at an arbitrary point in the amplifier A_2, fig. 1), plotted as a function of the time t.
a) Without counter-measures, the black level would fluctuate slowly as a result of the presence of low-frequency components in the photo-current of the image iconoscope.
b) By means of "clamping", the black level is fixed at the beginning of each line.

In addition, at the beginning of each line, the control grid of one of the tubes of amplifier A_2 (fig. 1) is earthed for a short moment ("clamping"), by means of an electronic switch.

The clamping circuit (*fig. 3*) is made up of four diodes, which are so arranged that they are conducting only if point A has a positive and point B has a negative potential. In that condition, the control grid g_1 is brought to earth potential. At the beginning of each line, a multivibrator (M_2) applies a positive pulse to A and a negative pulse to B, and thus each time reduces the signal level at g_1 to zero. The multivibrator M_2 is controlled by another multivibrator (M_1), which in turn is triggered by the line-synchronizing pulses of the 625-line system. With the aid of these multivibrators the most favourable position and width of the pulses applied to A and B can be adjusted.

By thus fixing the black level for each line, not only is the disturbance due to the low-frequency component in the photo-current largely eliminated, but also low-frequency disturbances of different origin, such as hum (from camera or amplifiers), and spurious signals in the vertical direction.

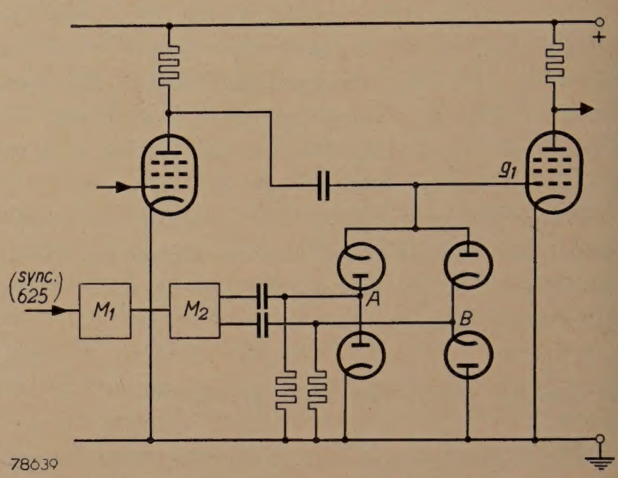

Fig. 3. The clamping circuit used, incorporated between two pentodes of the amplifier A_2 (fig. 1). M_1, M_2 multivibrators. g_1 control grid, which is periodically restored to earth potential via the four diodes.

Interference between the two numbers of lines

The second difficulty encountered is caused by the fact that the traced lines (405) and the scanned lines (625) have a tendency to form interference patterns on the target of the camera tube. This is to be attributed to the co-existence of various factors. Essentially it is caused by the changes in the mutual positions of the two line-types: at one place a scanned line will more or less coincide with a traced line, at another place it will come approximately in between two traced lines. In the latter case the signal obtained will be the weaker of the two. As a consequence of this, an interference pattern consisting of horizontal dark and light bands will be superimposed on the 625-line pattern.

At first sight one would expect the number of dark bands to equal the difference between the numbers of lines, i.e. $625 - 405 = 220$ (approx. 10% of which will be invisible because of the periodic frame blanking).

Such an interference pattern, however, is hardly discernible as far as the image iconoscope is concerned, but another pattern, containing about 100 dark bands, does occur. The cause of this lies in the fact that the "scanning sensitivity" of a target element is greatest just before and smallest immediately after scanning; we define the "scanning

sensitivity" here as the reciprocal of the ratio of the charge supplied by the photo-current in a short time interval to the resultant charge contributed to the signal current.

For the output signal we have

$$i_{sign} = [\int_{t_1 - 1/25}^{t_1} s(t) \cdot i_{ph}(t) \cdot dt]/^1/_{25}$$

in which i_{sign} is the signal current at the moment of scanning (t_1), and $s(t)$ and i_{ph} are the scanning sensitivity and the photo-current respectively, at a moment t.

The occurrence of an interference pattern with approximately 100 dark bands is illustrated by *fig. 4*, in which the measured relative sensitivity is plotted as a function of the time. A description of the method of measurement is given in the caption. This curve clearly shows that whatever is traced during the *last* $^1/_{50}$ *second before scanning*, contributes far more to the output signal than that traced $^1/_{50}$ second previously.

Fig. 4. Sensitivity s of a target element of the image iconoscope, plotted as a function of time t. After each scanning of an element (t_1, $t_1 + {}^2/_{50}$, ...), s drops from its maximum value (represented here as 100%) to its minimum value. At $t_1 + {}^1/_{50}$, neighbouring elements are scanned by the interlaced frame.

The curve was measured as follows. Light flashes of duration 4 milliseconds were projected on a small area of the photocathode with a repetition frequency of 25 c/s. The time lag between the illumination and the scanning of the corresponding area of the target was varied and the output signal of the image iconoscope measured as a function of this time lag, at constant values of photo-current and scanning current. For different values of these currents, slightly different curves were found, but all having a similar form, viz. a sudden drop of s on scanning, and an increase beginning midway between two successive scannings.

If the tube is used as a line converter, therefore, each scanning produces a signal which is mainly derived from the *immediately preceding* frame tracing. The lines of one scanned frame will thus mainly interfere with the lines of the immediately preceding traced frame. This causes an interference pattern with $\frac{1}{2}(625-405) = 110$ dark bands (about 100 of which are visible). This "secondary" pattern, as has been mentioned already, predominates over the primary interference.

A satisfactory method of removing this interference pattern was evolved, which consists in tracing the lines on the picture tube of such a thickness that they overlap. Although this involves a certain loss of definition in the vertical direction, the definition in the horizontal direction remains unimpaired if the thickening of the lines is effected by "spot wobbling".

This is a small vertical oscillation superimposed on the normal rectilinear movement of the light-spot, so that the latter traces sinusoidal lines. The amplitude is about twice the line separation, and the frequency is chosen so high that the oscillation is not visible.

In our line converter, spot wobbling is effected with the aid of a simple valve oscillator using a pentode, and an additional pair of deflection coils on the neck of the picture tube. These coils are incorporated in the oscillatory circuit of the oscillator. The frequency is approx. 10 Mc/s, so that one line includes roughly 600 sine-wave cycles. The amplitude is variable by adjusting the screen-grid voltage of the pentode.

In June 1953, after the London broadcasts, some programmes from Paris were also relayed to the Netherlands. It was then found that the above-mentioned interference occurred to a far less degree with a conversion of a larger number of lines into a smaller number (819 into 625). Even without spot wobbling, no disturbing interference was discernible.

Further examination of the origin of the "secondary" interference pattern

Fig. 5 shows four different "cross-sections" of the lines on the target plate, marked *1*, *2*, *3* and *4*. AB, CD and EF are cross-sections of lines of the first *traced* frame, $A'B'$, $C'D'$ and $E'F'$ of lines of the second (interlaced) frame; PQ, RS, etc. are cross-sections of lines of the first *scanned* frame, and $P'Q'$, $R'S'$ etc. of lines of the second (interlaced) scanned frame.

For simplicity, the following assumption are made: the two traced frames are exactly complementary (thus $A'B' = BC$, etc.), and the two scanned frames are also complementary ($P'Q' = QR$, etc.); further, the upper *traced* line and the upper *scanned* line start at the same level (both A and P are at the level h_1), and the number of traced lines to the number of scanned lines is in the ratio of 3 : 4. From this last assumption it follows that after three traced lines (i.e. four scanned lines) the initial condition is restored, so that the situation between h_1 and h_2 is representative of the whole target. Furthermore, we shall, for the time being, assume that the afterglow of the picture tube is zero.

Fig. 5 shows on which scanned lines a signal of the immediately preceding traced frames is obtained, as well as the ratio of the corresponding signal strengths. This depends on the extent to which the odd-numbered scanned lines (under *2*) overlap the odd traced lines (under *1*), and the overlap of the even-numbered scanned lines (under *4*) on the even traced lines (under *3*). The extent of the overlap in each case is shown by the shaded parts in fig. 5; the size of each shaded area is a measure of the signal strength at the corresponding scanned line. We see that at the levels h_1 and h_2 a strong signal is produced and between these, at a level h_m, a weak signal.

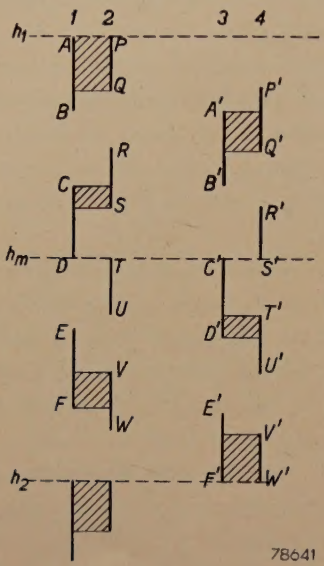

Fig. 5. An illustration of the occurrence of the "secondary" interference pattern. *AB*, *CD* and *EF* are "cross-sections" of lines *traced* on the target of an odd-numbered frame, and *PQ*, *RS*, *TU* and *VW* are cross-sections of odd-numbered *scanned* lines. The cross-sections *A'B'*, *C'D'*, etc. and *P'Q'*, *R'S'*, etc. similarly correspond to even-numbered frames. In this example it is assumed that *P* lies at the same level as *A* (at the level h_1), and that the ratio of the number of traced lines to the number of scanned lines is 3 : 4 (thus below h_2 the band h_1-h_2 is repeated), and the interval between the lines is equal to the line width ($AB = BC = A'B'$, etc. and $PQ = QR = P'Q'$, etc.). The size of each shaded area is approximately a measure of the signal strength per scanned line. Strong signals are thus produced at h_1 and h_2, and weak signals between them, at h_m. This explains the occurrence of light bands in the picture at h_1 and h_2 and dark bands at positions corresponding to h_m.

When an image is built up from these signals, it will exhibit light bands at heights corresponding to h_1 and h_2, with dark bands in between. This applies to both interlaced frames. The number of dark bands is equal to the difference between the number of lines per frame; this is what we have defined above as the "secondary" interference pattern. (The "primary" pattern, with double the number of dark bands, viz. the difference between the number of lines per *complete picture*, is lacking in fig. 5. This is a consequence of the assumption that the tracing lines are of the same width as the interspacing, although actually they are slightly narrower. This pattern shows light bands at h_1 and h_2 as in the secondary interference, but in addition there is also a light band at h_m. The latter is formed because the line *R'S'* is scanning the traced line *CD*. This produces only a weak signal, since *CD* does not belong to the immediately preceding traced frame; for this reason primary interference is not very pronounced with the image iconoscope.)

The *intensity* of the secondary interference pattern depends on the time interval between tracing and scanning, i.e. on the time lag between the tracing beam in the picture tube and the scanning beam in the camera tube. It also depends on the afterglow or decay time of the phosphor. This can be clarified if we examine more closely what actually happens on the surface elements of the target.

Consider first the surface elements which receive their charges from, say, an "odd numbered" tracing frame. These surface elements can belong to either of two groups: elements that will be scanned in the next scanned frame, and elements for which this will take place in the subsequent (interlaced) scanned frame. If the time lag between tracing and scanning for the first group is Δt, then it is $\Delta t + {}^1/_{50}$ sec for the second group. The elements of the two groups are by no means uniformly distributed over the target plate; there are places where elements of the first group predominate, as well as places with a majority of elements of the second group, and furthermore there are places where both groups are represented at about equal strength. The places with mainly elements of one group correspond to the bright bands of the primary interference pattern, since there the scanned lines coincide more or less with the traced lines, so that the time lag has in the main the same value (Δt in the first, third, etc. bright band; $\Delta t + {}^1/_{50}$ sec in the second, fourth, etc. bright band).

The same applies to an "even-numbered" tracing frame. For this, too, there are certain areas of the target where elements with time-lag Δt prevail and which, therefore, correspond to the first, third, etc. bright bands in the picture; and areas where the predominant time-lag is $\Delta t + {}^1/_{50}$ sec, corresponding to the intermediate bright bands, as well as the mixed areas corresponding to the dark bands of the primary interference pattern.

Consider now the photo-current i_{ph} which impinges on an element ΔS, having a time-lag Δt. In *fig. 6*, i_{ph} is plotted as a function of the time. At an instant t_1, the tracing beam in the picture tube passes a surface element of the fluorescent screen, corresponding to ΔS. This element begins to emit light, at an intensity which decreases according to the afterglow characteristic of the particular phosphor. The photo-current decreases correspondingly (fig. 6*a*). The target element under consideration is scanned at the instant $t_2 = t_1 + \Delta t$. In fig. 6*b* the same is shown for an element having a time-lag $\Delta t + {}^1/_{50}$ sec; at $t = t_3$ the photo-electrons begin to impinge upon the target element, and at $t_4 = t_3 + \Delta t + {}^1/_{50}$ sec the scanning beam passes the element.

The thin line in fig. 6 represents the scanning sensitivity of a target element (cf. fig. 4). The signal can be found from this diagram by integration of the product of s and i_{ph} over a period of ${}^1/_{25}$ sec, but without going into this further, it is apparent that the signal produced in the case of fig. 6*a* is stronger than that of fig. 6*b*, since in fig. 6*a* the state of high sensitivity coincides with a high momentary value of the photo-current, while the contrary is the case in fig. 6*b*.

This difference in signal strength, which causes the secondary interference pattern, is obviously dependent on Δt, the value of which may vary between 0 and ${}^1/_{50}$ sec. If one reduces Δt, the signal strength in fig. 6*a* decreases and that in fig. 6*b* increases, and at a certain value of Δt both signals will be equally strong and the secondary interference pattern will disappear. Secondary interference could be avoided in this way; in practice, however, the earlier mentioned method of

spot wobbling is more satisfactory, since then Δt can be made as large as possible, so that the effect of movement blurring is reduced to a minimum.

To complete this account, we should mention still another cause of the occurrence of the secondary interference pattern, viz. the slight overlapping of the lines of the interlaced frames. As, however, this effect is of minor importance in an image iconoscope, we shall not pursue it further here.

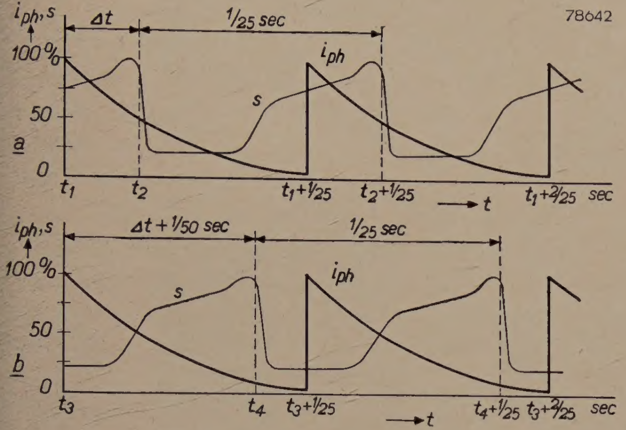

Fig. 6. Effect of the time lag Δt between tracing and scanning. The photo-current i_{ph} impinging upon a target element, and the sensitivity s of this element are plotted as functions of time (i_{ph} follows the afterglow characteristic of the phosphor, and s is the characteristic shown in fig. 4; both quantities are represented on an arbitrary scale).

In (a), a high sensitivity coincides with a high momentary value of i_{ph}, which is not the case in (b). This is the reason why a stronger signal is produced in case (a) than in case (b).

Beats caused by inequality of the frame frequencies

The third difficulty mentioned occurs if there is a slight difference between the picture frequencies of the two TV systems. As a rule, the mains frequency — nominally 50 c/s in Europe — is selected for the frame frequency (twice the picture frequency). If, however, the grid systems of the countries in question are not interconnected — and the British system is not linked up with the continental ones — small differences in the picture frequency will occur. The time lag between tracing and scanning of the target in the camera tube will then change continuously. This causes the output signal strength of the camera to fluctuate with a frequency equal to the difference between the two picture frequencies. In the final 625-line picture this is visible as a brightness fluctuation having the difference frequency.

If the picture frequencies are unequal, it is moreover possible that some of the aforementioned disturbing effects will be noticeable. If, due to inadequate clamping, the low-frequency components of the photo-current have not been completely eliminated, a dark horizontal band is seen across the screen, and also the amount of movement blurring and the intensity of the secondary interference pattern fluctuate.

By using suitable values of the mean photo-current and the beam current of the image iconoscope, these difficulties can be largely eliminated. More effective, however, is *the exact synchronizing of the two picture frequencies*, i.e. during the relay, the 625-line system is made to operate, independently of the continental electricity supply, with the British picture frequency, which is determined by the frame-synchronizing pulses in the British signal.

During the relays of June 1953, synchronized frame frequencies were used. At certain moments, however, when the chain of link transmissions between London and Breda was disturbed, the line converter temporarily received no frame-synchronizing pulses, or only badly distorted pulses, with the result that on the 625-line receivers the picture became unsteady, which is very unpleasant for the viewers. In such cases the exact synchronization of the picture frequencies was dispensed with and the difficulties reduced in the manner described above, by selecting the most suitable adjustment for the mean photo-current and the beam current.

Description of the equipment used

The line converter is shown in *fig. 7*. It was installed in duplicate in a trailer which was situated, for the relay of June 1953, at the foot of a church tower in Breda (see figs. 2 and 3 of the article referred to in [1])). On top of the tower were a beam receiver, directed to Antwerp, and two transmitters beamed at Lopik and Eindhoven.

The equipment consists of two parts: the 405 (or 819)-line section, which comprises the picture tube and its auxiliary components, and the 625-line section, viz. the camera tube and its associated equipment. Each is housed in three portable units (*1*, *2*, *5* and *3*, *4*, *6*, respectively, fig. 7).

The picture tube and its auxiliary equipment

The picture tube is of a special construction. It has a flat window of only 12 cm diameter and produces a picture of very high definition: in the centre the resolving power is more than 900 lines. The tube was operated at an anode voltage of 25 kV and a mean beam current of approx. 40 μA. The phosphor employed (willemite) then produces a luminance [5]) of approx. 5000 nit (≈ 16 000 apostilb) in the brightest parts of the image; the average luminance is then ample to

[5]) 1 nit = π apostilb = 1 candela (international candle) per m² = 1 lumen per m² per unit solid angle.

Fig. 7. The six portable units, constituting the line converter used at Breda. Unit *1* contains the picture tube, the video-output amplifier and the oscillator for spot-wobbling. Unit *2* contains the first video amplifier, the saw-tooth generators for the picture tube and the controls. Unit *3* contains the camera and its image iconoscope, type 5854, two output valves for the deflection currents and a pre-amplifier for the picture signal. Unit *4* houses the second picture-signal amplifier, the saw-tooth generators and the controls. *5* and *6* are power-supply units. To the extreme right is a monitor.

permit the image iconoscope to operate without disturbing spurious signals.

The saw-tooth generator for the horizontal deflection can be set by means of a switch to 405, 819 or 625 lines (the last line-number makes it possible to test the equipment without a British or French signal being available).

It is essential that the synchronization of both deflection systems of the picture tube is very stable. For this reason the *horizontal* deflection circuit incorporates a flywheel circuit, which can be adjusted to any of the three TV standards. This flywheel synchronization considerably reduces the influence of pulse-shaped disturbances and of temporary irregularities in the line-synchronizing pulses [6]).

[6]) P. A. Neeteson, Philips tech. Rev. 13, 312-322, 1952.

This method, however, does not give satisfactory results if the incoming line-synchronizing pulses are slightly frequency-modulated (e.g. a modulation with 50 c/s from the mains supply to the synchronizing pulse generator). If this should occur, and flywheel synchronization is used, then the sides of the frame, and indeed all vertical lines of the picture, will be distorted. For this reason provision is made for cutting out the flywheel synchronization. During the transmissions of 1953 it was found that the synchronization pulses were nearly always good enough to permit flywheel synchronization.

In a method often used for synchronizing the *vertical* deflection, the synchronizing signals are applied to an integrating *RC* network. The voltage across the capacitor of this network undergoes a substantial change only during the frame-syn-

chronizing signal, and the passing of a certain critical value determines the moment when a frame change takes place. A simple method of this kind will not be adequate for a line converter, which has to give reliable operation at any of three TV standards each with a frame-synchronizing signal of different shape. Satisfactory results were achieved, however, by using a circuit with *double integration.*

It has been described how, by means of clamping, the black level of the 625-line signal was fixed. Something similar takes place with the incoming signal, by the aid of a clamping circuit which operates on the control grid of the output tube of the video amplifier preceding the picture tube. The back porch of the line-synchronizing signal is then used as a reference level. As, however, the incoming signal could not always be counted on having a well-defined back porch, it was necessary that this clamping too, could be cut out at will.

The camera tube and its auxiliary equipment

The camera (*3* in fig. 7) contains an image iconoscope [4]), type 5854, two output valves for the saw-tooth deflection currents and a pre-amplifier for the picture signal. The camera is provided with a Leitz "Elmar" lens, having a focal length $f =$ 58 mm and an aperture f : 3.5. With regard to the choice of the lens, it should be taken into account that the image reduction used here is only (5-6) : 1, which is, of course, far less than that for which normal camera lenses are designed. For line conversion, a lens turret and a view finder [7]) were unnecessary, so that the camera could be kept very small (fig. 7).

Owing to the high luminance of the light spot, the output signal of the image iconoscope was of such strength that no special provisions regarding the signal-to-noise ratio were required. It was thus possible to employ a pre-amplifier of a conventional type. This circuit is shown in *fig. 8.*

The first tube is a double-triode ECC 81, the two halves being connected in parallel in order to obtain a low equivalent noise resistance. (The equivalent noise resistance of a valve is the value of the resistance, which, if inserted in the grid circuit, would cause a noise output equal to that produced by the tube itself.)

In order to prevent the second tube, a pentode EF 80, from also contributing substantially to the noise, this tube has been connected up as a triode, in order to avoid the partition noise due to the random division of the cathode-current between screen-grid and anode. The control grid of this tube is connected, via a resistor R_1 of 0.68 MΩ, to the input, which causes a certain negative feedback. In itself, this does not improve the signal-to-noise ratio, but it permits the use of a higher input resistance which does produce a better signal-to-noise ratio.

The third and the fourth tubes are pentodes EF 80, connected in the usual manner, the latter tube being arranged as a cathode follower. From the cathode of this tube, the picture signal is fed to a second amplifier via a cable.

The high input resistance of the pre-amplifier causes a considerable attenuation in the higher frequencies. For this reason the second amplifier has been given a frequency-response that compensates for this attenuation. The clamping circuit incorporated in this amplifier has been dealt with earlier in this article.

---

7) Normal television cameras contain a view-finder either of the optical type (with large-aperture lens) or of the electronic type (small picture tube with associated components). Both types are fairly bulky in comparison with the other components of the camera.

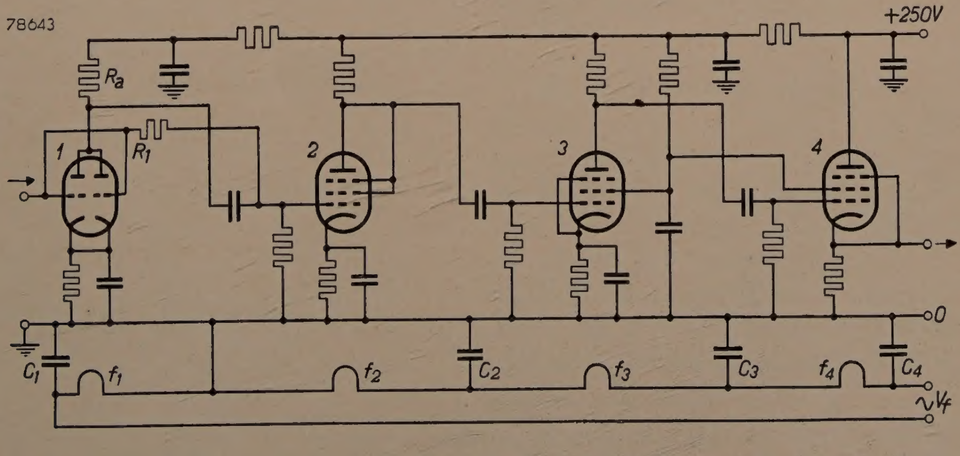

Fig. 8. Circuit diagram of the pre-amplifier in the camera. *1* double triode ECC 81 (the two sections connected in parallel) with anode resistor R_a = 4200 Ω. *2* pentode EF 80, connected as a triode. *3* and *4* normally connected pentodes EF 80, the latter operating as a cathode follower. R_1 (0.68 MΩ) negative-feedback resistor. The filaments (f_1, f_2, f_3, f_4) are connected in series (filament voltage V_f) and are earthed for high frequencies via the capacitors C_1, C_2, C_3 and C_4.

In the second amplifier, the blanking and synchronizing pulses are added to the picture signal, to form the complete video signal. These pulses are derived from a signal generator. The repetition-frequency of the frame-synchronizing pulses is governed by a sinusoidal auxiliary voltage. This voltage is derived, either from the saw-tooth current for the vertical deflection of the picture tube, or, when this is not feasible, from the mains. In the former case, the 625-line system is given the same picture frequency as the incoming signal, with the advantages outlined above.

The high speeds at which the photo-electrons hit the target in the image iconoscope render it fairly insensitive to stray electric and magnetic fields, but certain precautions are nevertheless required if maximum definition is to be attained. Especially the magnetic fields of the filament-current transformer and of the filament-current leads can be disturbing factors. For this reason the filaments of the pre-amplifier tubes are connected in series (fig. 8); so also are those of the output valves for the deflection currents. In this way the total filament current is considerably smaller, so that it was possible to locate the filament-current transformer away from the camera.

Some final observations

Very satisfactory results were obtained with the equipment described above. Some deterioration of the definition was, of course, unavoidable, but this was only slight. The gradation of the incoming signal was reproduced with great fidelity in the converted image, without gamma correction being necessary. Spurious signals from the image iconoscope were hardly discernible, thanks to the ample luminance of the intermediate optical picture (this would have been more difficult to attain with a *larger* picture tube). Another consequence of the high luminance was that the signal-to-noise ratio of the output signal was only slightly less than that of the incoming signal. Neither the grain, nor any other visible inhomogeneities of the phosphor presented any special difficulties.

Summary. A description is given of the line converter which was used to convert the British (405-line) television signal into a 625-line signal for transmission in the Netherlands and Western Germany on the occasion of the Coronation in London in June 1953. The apparatus was also capable of converting signals of the French standard (819 lines) into the 625-line system. The line converter uses a picture-tube to produce an intermediate optical image of the incoming signal. This image is viewed by an image iconoscope (type 5854) which scans it in the 625-line system. The disturbing effects which occur during this process are dealt with, as well as the means for eliminating them. The latter include: the use of a long afterglow phosphor in the picture tube, spot-wobbling in the picture tube, clamping of the black level in the output signal at the beginning of each scanning line, and the equalizing of the picture frequency of the 625-line system to that of the incoming signal (when the conditions are suitable). The picture tube has a screen of 12 cm diameter, the long afterglow phosphor being willemite. The luminance reaches a maximum value of 5000 nit. Its mean value is ample to ensure that the image iconoscope is almost free from spurious signals, and that the signal-to-noise ratio of the signal is only slightly diminished on passing through the line converter.

AN INSTRUMENT FOR MEASURING GROUP DELAY

by H. J. de BOER and A. van WEEL. 621.317.342.018.782.4:621.397.6

In radio receivers it is important that each frequency component of the audio signal is equally amplified, while phase shifts in the signal components of different frequencies have little effect on the quality. On the other hand, phase shifts in the video signal of a television receiver are very important; hence the transmission time, or delay of a signal passing through the receiver should be independent of frequency. An instrument with which differences in transmission time can be measured accurately to within 10^{-9} sec is described in this article.

Introduction

Phase delay

Distortion of several kinds may be introduced into an electrically transmitted signal by the transmitting network (cable, amplifier, transmitter, etc.). One type is associated with the phase delays at the different frequencies involved.

To define "phase delay", let us consider the case of a signal $A \cos(\omega t + \beta)$ applied to the input of a network; on reaching the output, this signal will have become

$$A' \cos(\omega t + \varphi + \beta).$$

where φ is the phase shift introduced by the network.

Writing

$$\tau_f = -\frac{\varphi}{\omega}, \quad \ldots \ldots \quad (1)$$

the output signal will be

$$A' \cos \{\omega(t - \tau_f) + \beta\}.$$

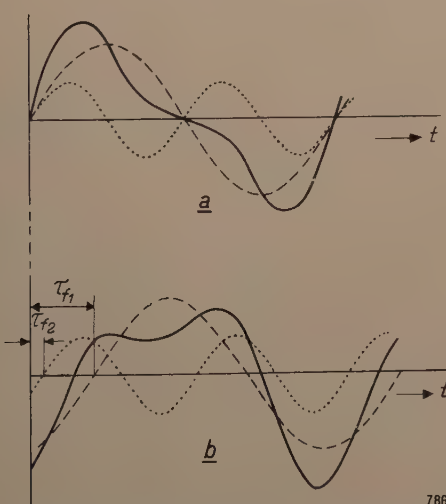

Fig. 1. Example of phase distortion. *a*) Input signal of a network. The signal contains components of angular frequency ω and 2ω as indicated by dotted lines.
b) Output signal of the same network. The phase delay τ_{f_1} of the component of angular frequency ω is assumed to exceed the phase delay τ_{f_2} of the component of angular frequency 2ω. It will be seen that phase distortion takes place.

Accordingly, the phase of the output signal at time $t_1 + \tau_f$ is the same as that of the input signal at time t_1; hence τ_f might be called the transmission time. It is generally known however as the phase delay.

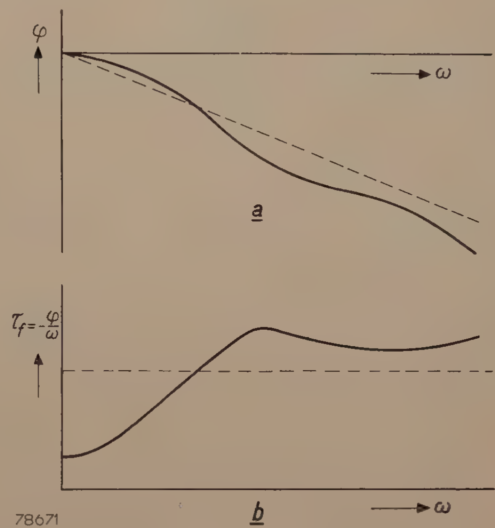

Fig. 2. *a*) Phase characteristics of a network that introduces phase distortion (full line), and that of a network which introduces no distortion (dotted line).
b) Phase delay characteristics derived from phase characteristics of (*a*).

The signal may be thought of as resolved into Fourier components which, if the phase delay depends on the frequency, will be displaced relative to one another when passing through the network. The distortion caused by these differences in delay is called phase distortion (*fig. 1*).

To avoid phase distortion, then, it is necessary to ensure that the phase delay is independent of frequency within the range defined by the Fourier components of the signal.

According to (1), this means that the phase shift φ introduced into a sinusoidal signal by the network must be directly proportional to the frequency within the range concerned.

Phase characteristics for networks with, and without phase distortion are illustrated in *fig. 2a*.

Fig. 2*b* shows that the delay is dependent on frequency in the first case, but not in the second.

Modulation phase delay

With a modulated carrier-wave signal the situation is different. Consider *figures 3a* and *b* which illustrate respectively the phase characteristic and the amplitude characteristic (amplitude gain a as a function of the angular frequency) for a typical radio-frequency network.

Let us assume that a carrier wave (angular frequency ω_0), whose amplitude is modulated sinusoidally to a depth m at a frequency $\omega_m/2\pi$, is applied to the network concerned. Such a signal (apart from a constant factor) is given by

$$S_i = (1 + m \cos \omega_m t) \cos \omega_0 t =$$
$$\cos \omega_0 t + \frac{m}{2} \cos (\omega_0 + \omega_m) t + \frac{m}{2} \cos (\omega_0 - \omega_m) t. \quad (2)$$

According to (2) this signal can be resolved into three components that will, in passing through the network, attain values that can be deduced from diagrams 3*a* and *b*. At the output of the network a signal corresponding to

$$S_u = a_0 \cos (\omega_0 t + \varphi_0) + a_1 \frac{m}{2} \cos \{(\omega_0 + \omega_m) t + \varphi_1\} +$$
$$+ a_2 \frac{m}{2} \cos \{(\omega_0 - \omega_m) t + \varphi_2\} \quad . \quad . \quad . \quad (3)$$

is thus produced.

A trigonometrical conversion of the above (see appendix) shows that the expression for S_u represents a carrier-wave with an angular frequency

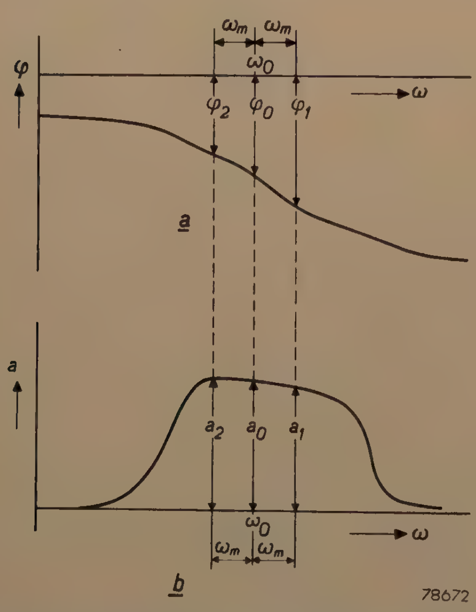

Fig. 3. Phase characteristic (*a*) and amplitude characteristic (*b*) of a typical band-pass network for high frequencies.

ω_0, whose amplitude is also modulated periodically at a fundamental frequency $\omega_m/2\pi$. We are not at present concerned with the higher harmonics also produced during this process.

It can be seen from the derivation in the appendix that if the original depth of modulation is small ($m \ll 1$), the fundamental component of the modulation is displaced through an angle ψ with respect to the modulation of the input signal, ψ being given by:

$$\tan \psi = \frac{a_1 \sin(\varphi_1 - \varphi_0) - a_2 \sin (\varphi_2 - \varphi_0)}{a_1 \cos(\varphi_1 - \varphi_0) + a_2 \cos (\varphi_2 - \varphi_0)}. \quad (4)$$

The time-dependent factor $\cos \omega_m t$ in the modulation of the input signal is thus converted into $\cos \omega_m (t + \psi/\omega_m)$ in the output signal; hence the "modulation phase delay" is:

$$\tau_{fm} = -\psi/\omega_m. \quad . \quad . \quad . \quad . \quad . \quad . \quad (5)$$

Phase distortion takes place in a modulation-transmitted signal if the modulation phase delay depends on the frequency of modulation. According to (5), then, a curve representing the phase shift ψ (defined by (4)) as a function of ω_m, for the band-pass sections of a television receiver (R.F. and I.F. stages), should be a straight line passing through the origin. In these circumstances the modulation phase delay $-\psi/\omega_m$ takes the place of the "normal" phase delay $-\varphi/\omega$ described earlier (see equation 1).

To study the effect of phase distortion in television receivers, we require a sufficiently accurate method of measuring differences in normal phase delay (in the video stage) and differences in modulation phase delay (in the R.F. and I.F. stages).

In principle, this can be accomplished by plotting the phase characteristics of the networks concerned; normal phase delays can be derived direct from these characteristics (see (1)). However, for the determination of modulation phase delay from (4) and (5), that we shall now consider, the amplitude characteristics of the R.F. and I.F. stages are also required. Although the required characteristics can be measured at high frequencies (several tens of Mc/s) [1]), the results thus obtained are not accurate enough for our purpose. The values of φ_0, φ_1 and φ_2 derived from the phase characteristics are generally large in relation to the differences $\varphi_1 - \varphi_0$ and $\varphi_2 - \varphi_0$ which must be known in order that formula (4) can be applied.

[1]) See, e.g. G. Thirup, An instrument for measuring complex voltage ratios in the frequency range 1—100 Mc/s. Philips tech. Rev. **14**, 102-114, 1952.

An instrument (*fig. 4*) with which direct and very accurate measurements of the slope of the phase characteristic ($\mathrm{d}\varphi/\mathrm{d}\omega$ as a function of ω) can be made will now be described.

For a reason which will be explained later, the quantity

$$\tau_g = -\mathrm{d}\varphi/\mathrm{d}\omega \quad . \; . \; . \; . \; . \; . \quad (6)$$

is known as "group delay"; hence the instrument is described as a "group delay meter". Differences in the phase shifts associated with different frequencies can be established by integration (e.g. graphic integration) of the group delay.

Thus:

$$\varphi_1 - \varphi_0 = -\int_{\omega_0}^{\omega_0+\omega_m} \tau_g \,\mathrm{d}\omega \,, \quad . \; . \; . \; . \; . \quad (7)$$

A similar expression applies to $\varphi_2 - \varphi_0$.

The instrument is designed to measure group delay accurately to within 10^{-9} sec; according to an estimate by Ring [2]) this is the degree of accuracy which should be aimed at.

To give some idea of the basis of this estimate, it may be seen from (1) that at a frequency of 5 Mc/s (the highest frequency in a video signal for 625-line television) a phase difference of 2π radians between signals at the input and output of a network corresponds to a phase delay of 200×10^{-9} sec.

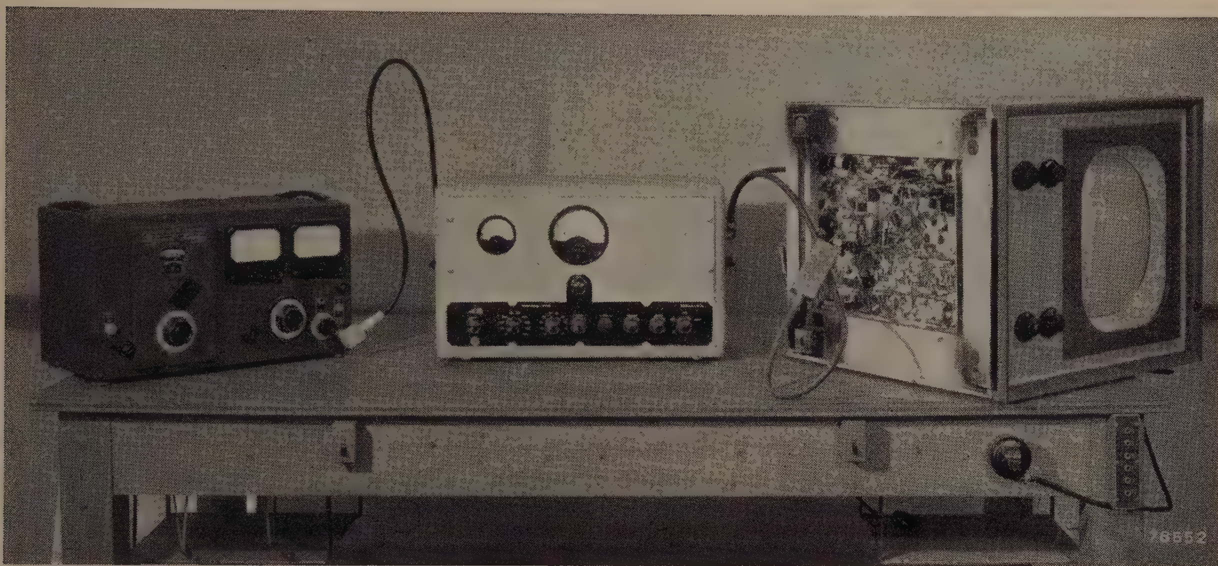

Fig. 4. The group delay meter (centre) as used for testing the R.F. and I.F. stages of a television receiver (on right of picture). At the extreme left is a signal generator producing the carrier wave required for the test. The equipment illustrated can be used for tests at carrier wave frequencies between 10 and about 100 Mc/s, the results being accurate to within 10^{-9} sec.

Group delay

The quantity $\tau_g = -\mathrm{d}\varphi/\mathrm{d}\omega$ is described as "group delay" by reason of its significance in the simple case of a frequency characteristic that is straight within the given range of interest. In this case:

$$\varphi_1 - \varphi_0 = -(\varphi_2 - \varphi_0) = -\tau_g \omega_m \,,$$

where τ_g is constant.

Substitution of the above in (4) gives us:

$$\psi = -\tau_g \omega_m, \quad . \; . \; . \; . \; . \; . \quad (8)$$

hence, according to (5)

$$\tau_{fm} = \tau_g. \quad . \; . \; . \; . \; . \; . \quad (9)$$

so that τ_{fm} remains independent of ω_m, provided that $\omega_0 + \omega_m$ and $\omega_0 - \omega_m$ are associated with a

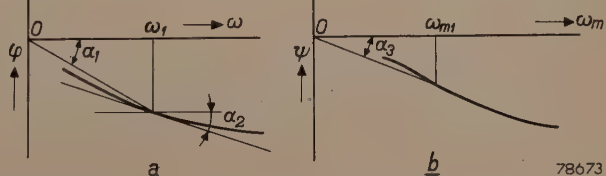

Fig. 5. *a*) Geometrical significance of phase delay and group delay. A phase characteristic is shown. The phase delay τ_f for an angular frequency ω_1 is $-\tan\alpha_1$ (see equation 1); the group delay τ_g for the same angular frequency is $-\tan\alpha_2$ (see equation 6).
b) The modulation phase delay characteristic for a certain carrier wave frequency. The angular frequency of modulation ω_m is plotted on the abscissa. The modulation phase delay at a modulation frequency ω_m corresponds to $-\tan\alpha_3$ (see equation 5) and so has in this graph the same mathematical significance as τ_f in (*a*).

[2]) D. H. Ring, The measurement of delay distortion in microwave repeaters, Bell Syst. tech. J. 27, 247-264, 1948.

portion of the phase characteristic which is adequately straight. Accordingly, a modulation signal comprising components with angular frequencies ω_m within this range will pass through the network with a delay τ_g without distortion.

A certain mathematical significance, as demonstrated in *fig. 5* (see caption), can be assigned to the different delays introduced.

Measurement of group delay

Let us assume that a signal of angular frequency ω is applied to a network whose group delay (i.e. slope of the phase characteristic) is to be determined at that angular frequency. The signal is modulated at an angular frequency, $\omega_m = p$, which is so low that the phase characteristic associated with any angular frequency band of width $2p$ may be considered straight.

The phase shift ψ associated with p and introduced into the modulation by the network will be denoted by ϑ, so that from (8),

$$\vartheta = -\tau_g p. \quad \ldots \ldots \quad (10)$$

At the fixed value p, then, ϑ is a measure of the group delay to be determined. The measurement of group delay is thus reduced to a measurement of the phase shift introduced into the modulation signal of angular frequency p by the network [3]).

The choice of a suitable modulation angular frequency p is limited by conflicting requirements. According to (10) sensitive measurement necessitates a high value of p, by virtue of which a small variation in τ_g will produce a substantial variation in ϑ. On the other hand, a low value of p is required for accuracy, since the approximation of the phase characteristic to a straight line will be better for a smaller value of p. Equation (10), too, is a better approximation in these circumstances. A frequency $p/2\pi = 25$ kc/s has been adopted as a suitable practical value for the present instrument; hence, from (10), it will be necessary to measure phase variations of 0.01° in order to determine group delay differences of 10^{-9} sec. Accordingly, the main problem is to design a very sensitive phase meter.

Principle of the phase meter

A property common to oscillator circuits is used in the measurement of small phase differences.

In principle, an oscillator is an amplifier of which all, or a portion of the output is fed back to the input to form a loop. At a given frequency, stable oscillation is possible only if the phase shift introduced into a signal at this frequency as it passes round the loop is a multiple of 2π. Every oscillator circuit contains a frequency-determining element the essential feature of which is that it imparts to the signal a phase shift, dependent (usually very sharply) on the frequency, such that the phase condition is exactly satisfied at the desired frequency. The circuit will commence to oscillate at the frequency concerned, provided that the amplification at this frequency exceeds unity. The amplitude of the oscillation at first increases, but is limited by an accompanying decrease in amplification until unity is reached.

In simple oscillator circuits the amplifier valves themselves act as amplitude-limiting elements, since their effective slope decreases as the amplitude of the grid voltage increases. However, it will be seen that in the present case, a separate, carefully designed amplitude limiter is required.

If an extra phase shift is introduced in some way into an oscillating circuit, stable oscillation is possible only at a frequency so far removed from the original oscillation frequency that the phase shift in the frequency-determining element due to the frequency variation, compensates for the introduced phase shift; in this way the phase condition (that the total phase shift in the loop is a multiple of 2π) is again satisfied.

If the condition as regards amplification is also met at the new oscillation frequency, the circuit will continue to oscillate at this frequency. It will be seen, then, that a certain relationship exists between a phase shift introduced into a signal and the change in frequency thereby produced. This relationship is the basis of the phase meter used in the present instrument. Further details are given below and in *fig. 6*.

Block diagram of the group delay meter

The diagram depicted in fig. 6 includes a selective amplifier A, the pass-band of which covers the modulation frequency employed, $p/2\pi = 25$ kc/s. The output voltage of the amplifier is applied to a modulator B, to which is connected a signal generator G producing a carrier wave whose frequency $\omega/2\pi$ is variable to cover the pass-band of the network X. The output signal of the modulator passes through network X and is then rectified by the detector C. By connecting the output of the latter to the input of the amplifier, a feedback loop is formed, so that oscillation can take place at the frequency p. The amplifier is therefore referred to

[3]) This principle was first applied to the measurement of phase distortion in long distance telephone communication. See H. Nyquist and S. Brand, Bell Syst. tech. J. 9, 522-549, 1930.

below as the p-amplifier. Special measures are taken to ensure that the phase condition can be satisfied in the frequency band about p.

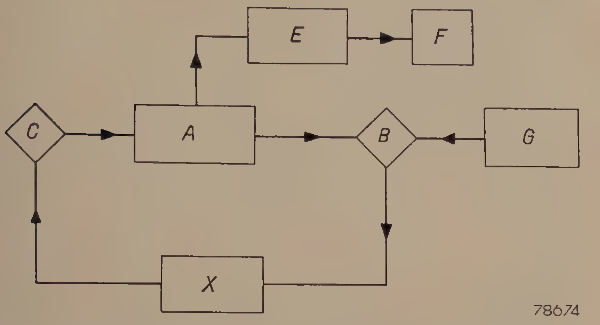

Fig. 6. Block diagram of the equipment used for measuring group delay as a function of frequency. Oscillation at a nominal frequency of 25 kc/s takes place in the loop formed by amplifier A, modulator B, network on test X and detector C. A phase shift in X produces a change in frequency which is converted by discriminator E into a voltage variation. The latter is measured by means of a valve voltmeter F. The signal generator G supplies a carrier wave of the frequency at which the behaviour of network X is to be investigated; this carrier wave is modulated with the oscillation frequency.

The exact value of the frequency of oscillation $p/2\pi$ is determined mainly by the frequency-determining element in the amplifier, but is also affected by the phase shift introduced into the modulated signal as it passes through network X. According to (10) the phase shift ϑ is related to the group delay of X at an angular frequency ω; hence a relationship exists between this group delay and the oscillation frequency. This relationship can be established in the following manner.

Relationship between group delay and frequency of oscillation

In the event of a change $\Delta\omega$ in the carrier-wave angular frequency ω, the group delay τ_g of X varies by $\Delta\tau_g$. At the same time, the angular frequency of oscillation changes from p to $p + \Delta p$, in such a way that the phase condition is still satisfied.

The phase shift of the modulation in network X thus changes (see equation 10) from $-p\tau_g$ to $-(p + \Delta p)(\tau_g + \Delta\tau_g)$, that is to say (neglecting the term $\Delta p\, \Delta\tau_g$) by an amount

$$\Delta\vartheta = -(p\Delta\tau_g + \tau_g\Delta p).$$

In the remainder of the loop, the phase shift changes by an equal amount but opposite in sign, $\Delta'\vartheta$. Let us now assume for a moment that the network X is short-circuited and the resultant loop is opened at the input terminals of the amplifier. If the phase characteristic of the network so obtained is straight in the region of 25 kc/s (it is easy to ensure that this is so), and its slope is $\mathrm{d}\varphi/\mathrm{d}\omega = -t_0$, we may write:

$$\Delta'\vartheta = -t_0\,\Delta p.$$

Evidently, t_0 represents the group delay of the open-circuit network (without X) for a signal modulating a 25 kc/s carrier wave. The quantity t_0 may be described as the inherent group delay of the instrument.

Equating $\Delta\vartheta$ and $-\Delta'\vartheta$, we find that:

$$\Delta\tau_g = -\frac{t_0+\tau_g}{p}\,\Delta p.$$

The measuring instrument is so constructed that $t_0 \gg \tau_g$; hence, ignoring the sign,

$$\Delta\tau_g = \frac{t_0}{p}\Delta p. \quad \dots\dots\dots \quad (11)$$

Since t_0 and p are known, $\Delta\tau_g$ can be determined [4]) by measuring Δp. The difference of phase delay $\Delta\tau_g$ thus established differs from τ_g itself only by an (unknown) constant.

A closer investigation shows that by using $\Delta\tau_g$ instead of τ_g in (7), and applying the result in (4) and (5), the modulation phase delay τ_{fm} is found, apart from the same constant. The omission of the constant does not invalidate the calculation since we are concerned only with differences in modulation phase delay.

Particulars of the instrument

The amplifier

The oscillation frequency should depend only on the group delay of the network on test; in the absence of such a network, then, the frequency should be constant.

In normal circumstances, highly selective circuits (e.g. crystal-controlled) are used in the design of stable oscillators. The salient feature of such circuits is that their phase characteristic is steep in the region of their resonant frequency (high t_0); the frequency variations produced by slight phase shifts within the circuit are accor-

[4]) The variation in group delay thus established relates to the portion of the loop through which the signal is transmitted on the carrier wave. Besides network X, this portion includes parts of the modulator and detector circuits. Special measures are then necessary to ensure that the amount contributed to the group delay by the modulator and the detector does not depend on ω in the range of frequencies concerned, so that only network X can produce a variation in the group delay. These measures involve the use of different modulators and detectors for different frequency bands.

dingly very small. This, however, applies to any phase variation, including the phase shift which is to be measured; hence this type of oscillator is not suitable for the present purpose. The sensitivity of measurement would be small, and, of course, the ratio of the effects of desired and undesired phase variations is not improved.

Stability of frequency in the oscillator must be obtained not by reducing the *effect* of undesired phase variations, but by avoiding such variations as far as possible.

This is accomplished by including amplifier stages of two different kinds in the instrument. The first kind of stages includes an anode circuit having an LC-circuit damped by a parallel resistor R. This LC-circuit, tuned to 25 kc/s, is the frequency-determining element of the oscillator. Apart from the sign, the phase shift produced by this amplifier stage is equal to the phase angle α of the anode impedance. A simple calculation shows that in the region of resonance:

$$\mathrm{d}\alpha/\mathrm{d}\omega = 2\,RC.$$

Accordingly, this also represents the amount contributed by the amplifier stage to the inherent group delay t_0 of the measuring instrument.

Secondly, a number of resistance-coupled amplifier stages with low anode resistance are used; these also cause slight phase shifts due to the valve and wiring capacitances in parallel with the anode resistance, but it is found that the magnitude of such shifts is not much affected by variations in the resistance and capacitance values, provided that a low value is chosen for the resistance. The stage gain is then small; hence several stages must be used to obtain the required overall gain. Variations in the phase shift that may occur within this portion of the instrument are so small that they may be ignored, and also the total contribution of the resistance-coupled amplifier stages to the inherent group delay t_0 of the instrument is so insignificant, that t_0 may be taken as equal to the contribution of the tuned stage only. Hence (see above),

$$t_0 \approx 2\,RC.$$

The value of RC is so chosen that $t_0 = 60$ µsec. The requirement $t_0 \gg \tau_g$ is thus satisfied for practical values of τ_g, and at the same time adequate sensitivity is maintained.

The amplitude limiter

Since an amplitude-limiting element in an oscillator cannot be linear, it inevitably introduces harmonics of the oscillation into the circuit. If a signal component at twice the fundamental frequency, as well as the fundamental itself, passes round the loop and reaches the input of the limiter, a beat frequency will be produced at the output with the fundamental frequency $p/2\pi$. This is known as conversion.

In general, this undesired beat signal will not be in phase with the desired signal; hence the resultant signal of frequency p (the p-signal) suffers a phase shift the angle of which will depend on the amplitude and phase of the undesired signal. If this phase shift were the same for all the frequencies within the measuring range, an equal amount would be added to each of the values of $\Delta\tau_g$ read from the instrument; this would not matter, since we are concerned only with group delay differences. Unfortunately, however, the amplitude of the undesired signal, and with it the effect on the phase of the resultant signal, will depend on the self-adjustment of the amplitude limiter, which will be such that the amplification of the p-signal by the loop is exactly unity. Since the amplification of the p-signal in the X-network will not as a rule be constant over the entire measuring range, the effect of the undesired p-signal will also vary.

Two measures have been adopted to limit this interference. Firstly, an almost distortionless amplitude limiter is used, and secondly the selective circuit included in the amplifier substantially attenuates the higher harmonics.

The discriminator

Frequency variations are measured by means of a frequency discriminator, producing at its output a D.C. voltage which is proportional to the difference between the frequency of the signal applied to the input and a certain fixed frequency. At the values of t_0 and p employed, a variation in group delay of 10^{-9} seconds corresponds to a frequency variation of about 0.5 c/s (see equation (11)); hence the fixed frequency must remain constant to within considerably less than 0.5 c/s if the group delay is to be measured accurately to within 10^{-9} sec. Moreover, the discriminator must be adequately sensitive.

To satisfy the latter requirement, the output voltage of the discriminator (which is directly proportional to the group delay variations to be determined) is measured with a valve voltmeter calibrated directly in nanoseconds (10^{-9} sec). The four measuring ranges covered by the voltmeter correspond to 0—1000, 0—300, 0—100 and 0—30 nanoseconds.

"Delay switching"

If an oscillation is produced in the loop in the absence of an unknown network X, the amplifier can be so tuned that the oscillation frequency coincides with the fixed frequency at which the output voltage of the discriminator is zero; measurement on an unknown network subsequently introduced into the circuit then produces the absolute group delay of this network. But we are concerned with variations in the group delay within a certain range of frequencies, rather than with the absolute value. If the absolute delay is relatively long (e.g. 500×10^{-9} sec) and the variations amount to no more than a few times 10^{-9}, the latter would have to be read from the 1000×10^{-9} sec scale.

To overcome this difficulty, means are prodived whereby known phase shifts can be introduced into the amplifier. This is accomplished quite simply by connecting different capacitors in parallel with a known resistance. A phase shift $\Delta\vartheta$ in the measuring instrument affects the oscillation frequency in exactly the same way as a change $-\Delta\vartheta/p$ in the group delay of the unknown network (see equation (10)). It is thus possible to "switch out" a known group delay. The instrument is so designed that group delay can be switched out in steps of 100×10^{-9} and 10×10^{-9} sec.

Testing circuits containing a detector

Many of the circuits to be tested (e.g. television receivers) include a detector and, when this is so, the detector normally included in the measuring instrument can be omitted; for example, the equipment illustrated in fig. 4 does not include a detector.

A detector in the circuit on test is usually followed by another network — in television receivers, the video stage — through which the signal passes before reaching the p-amplifier. If the phase characteristic of this network is not horizontal in the region of the angular frequency p, it affects the value of t_0 (see equation 11). The video stage of a television receiver, however, is a broad-band amplifier containing no selective circuits; hence its phase characteristic is so flat that it does not seriously affect t_0. Accordingly, equation (11) continues to apply to delay variations in that portion of the receiver in which the carrier wave is modulated by the signal.

A signal which, in the set on test, passes through an uneven number of valves after leaving the detector, would be exactly π radians out of phase after travelling once round the measuring circuit, so that oscillation would not take place if special measures were not taken to correct this phase shift. Accordingly, a special switch is provided on the instrument with which the phase can be increased by π radians.

The arrangement used for testing a television receiver is illustrated in fig. 4.

Tests at video frequencies

Whereas the preceding arguments are based on the assumption that the p-signal travelling through the circuit on test is always in the form of modulation, the modulator really produces, apart from the modulated carrier wave, other signals, including one with an angular frequency of p. After passing through the circuit on test this direct p-signal will affect the phase of the desired signal in a manner that, since it cannot be predicted, may well upset the group delay measurement.

During measurements on band-pass portions of the circuit on test, the direct p-signal in this circuit will be so attenuated that it cannot reach the p-amplifier, but if the pass band of the network also includes angular frequency p, as it does in video-frequency amplifiers, this suppression will not take place. In these circumstances, special measures must be taken to ensure accuracy in the measurement. For this reason, an adaptor has been designed which, combined with the group delay meter described, enables measurements at frequencies between about 0.1 and 10 Mc/s to be carried out.

The adaptor contains a balanced modulator, which does the work of the modulator in the original equipment, and a balanced detector. In principle, these balanced circuits should produce no p-signal at the output [5]), but in fact the suppression is never complete. The phase of the final signal is most seriously affected when the phase difference between the residual signal at the output of the detector and the desired signal travelling as modulation through the circuit on test is $\pi/2$ (*fig.* 7).

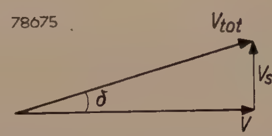

Fig. 7. Error introduced by an interfering signal V_s. The desired signal is V and the total signal V_{tot}. The phase difference δ between V and V_{tot} reaches a maximum when V_s and V are about $\pi/2$ out of phase, but is zero (and thus introduces no error) when V and V_s are either in phase, or in antiphase.

On the other hand, no error is introduced when the phase difference between the signals is either 0 or π; hence it is essential to ensure that the difference obtained corresponds as closely as possible to one of these two values. Further analysis has shown that this can be accomplished by including in the modulator and detector special features whereby the components of angular frequency p, produced by the two push-pull valves in their

---

[5]) See, e.g. F. A. de Groot and P. J. den Haan, Modulators for carrier wave telephony, Philips tech. Rev. 7, 83-91, 1942.

common signal, are kept as far as possible in anti-phase (phase balancing).

It is found by experiment that a residual signal constituting 1% of the desired signal introduces a perceptible error into the test results if produced by a disturbance of the phase balance, whereas a similar signal produced by a disturbance of the amplitude balance scarcely affects the results.

Fig. 8. Combination of group delay meter and video adaptor (top) used for group delay measurements in the frequency band between about 0.1 and 10 Mc/s.

In the circuit described here, as in the resistance-coupled stages of the amplifier, only resistors of low value are employed; hence there can be little variation in the phase balance when once adjusted.

The adaptor also contains a selective test amplifier, tuned to angular frequency p, which can be used to control and check the balance of the modulator and the detector when connected to the output of either of these units.

The combination of a group delay meter and an adaptor is illustrated in *fig. 8*. This combination is used for group delay measurements in the frequency band of 0.1 to 10 Mc/s, and the group delay meter without adaptor for similar measurements in the band of 10 to about 100 Mc/s. In principle, there is no maximum limit to the frequencies for which the above method can be employed, but in practice a limit is imposed by the fact that suitable modulators and detectors must be built for each frequency band (see note [4]). A rather complex relationship exists between the lower frequency limit and the magnitude of p. Measurements at frequencies down to about 60 kc/s have been achieved with certain precautions.

In order to calculate the phase delay it is necessary to extrapolate the measured group delay differences to $\omega = 0$. Like modulation phase delay, the phase delay thus calculated lacks an additive constant.

Some test results

As a general example of the kind of information obtainable with the equipment described here, curves plotted from some of the results are shown. The first of these relate to tests on a television receiver; the R.F. and I.F. stages of this receiver were tested together and a curve was constructed representing the difference of the group delay from that at the carrier wave frequency of the television transmitter (in this case *Lopik* at 48.25 Mc/s) to which the receiver was tuned (*fig. 9a*). This curve, together with the amplitude characteristics of the R.F. and I.F. stages (which were known), was used to compute the modulation phase delay τ_{fm} (apart from an additive constant). It is shown as passing through the origin in fig. 9*b*.

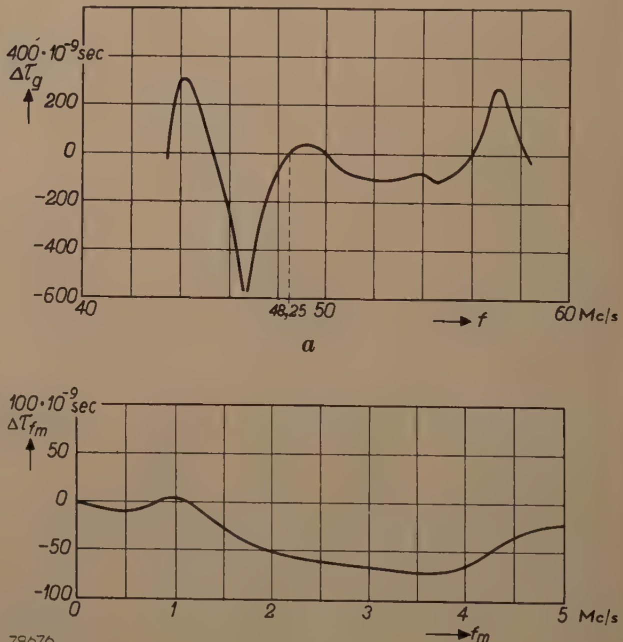

Fig. 9. Group delay characteristics of the combined R.F. and I.F. stages of a television receiver. The differences $\Delta\tau_g$ with respect to the group delay at the carrier wave frequency of the Lopik television transmitter (48.25 Mc/s) are shown. *b*) Modulation phase delay of the combined R.F. and I.F. stages of the television receiver. The quantity $\Delta\tau_{fm}$, derived from the group delay characteristic (*a*), is plotted as a function of the modulation frequency, taking into account the amplitude characteristics of the parts of the network on test.

Another curve, representing the group delay as measured in the video stage between the detector and the picture tube of the same television receiver, is illustrated in *fig. 10*. This illustration also includes the normal phase delay characteristic derived from the group delay characteristic.

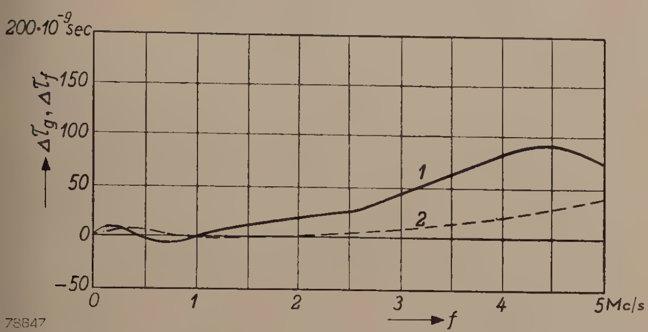

Fig. 10. Delay characteristics of the video stage of a television receiver. Curve *1* represents the differences in group delay determined by direct measurement, and curve *2* the differences in phase delay derived from *1*.

The group delay characteristic of the complete receiver, i.e. for all stages between the aerial terminals and the picture tube, will be seen in *fig. 11*. Two modulators were used to plot this characteristic, one modulating the video signal with an angular frequency p, and the other modulating a high-frequency carrier wave with the modulated video signal, which is then applied to the aerial terminals. The video signal after detection in the video detector of the receiver, passes through the video stage of the latter and is in turn detected by the detector included in the adaptor. The phase delays derived from the measured group delay characteristic are also shown in the illustration (fig. 11). Also included, as a check, are

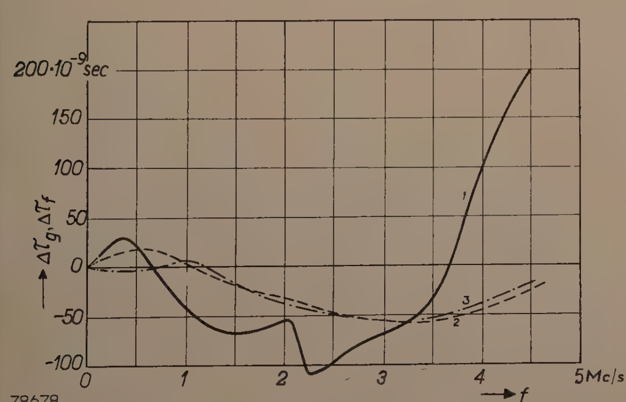

Fig. 11. Delay characteristics of a complete television receiver (from aerial terminals to picture tube). Curve *1* represents the differences in group delay $\Delta\tau_g$ determined by direct measurement, curve *2* the differences in phase delay $\Delta\tau_f$ derived from *1*; curve *3* also represents $\Delta\tau_f$, this time determined as the sum of $\Delta\tau_f$ for the video stage (fig. 10) and $\Delta\tau_{fm}$ for the R.F. and I.F. stages (fig. 9*b*).

the same phase delays computed as the sum of the modulation phase delays in the R.F. and I.F. stages (fig. 9*b*), and the phase delay in the video stages (fig. 10).

Lastly, the delay characteristics of an amplifier specially designed for a television studio are illustrated in *fig. 12*. It will be seen that the phase delay characteristic thus obtained is very flat and hence that the amplifier concerned introduces hardly any phase distortion.

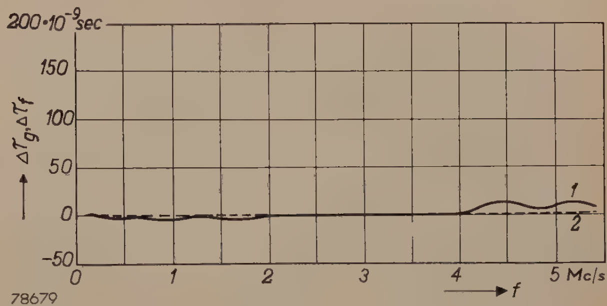

Fig. 12. Delay characteristics of a special video amplifier designed for use in television studios. Curve *1* represents the measured differences in group delay, and curve *2* the differences in phase delay.

Appendix. Derivation of formulae for modulation phase delay

When applied to the input of a high-frequency network, a modulated carrier wave as defined by formula (2) produces at the output a signal of the form (formula (3), slightly rearranged):

$$S_u = a_0 \cos(\omega_0 t+\varphi_0) + a_1 \frac{m}{2} \cos\{(\omega_0 t+\varphi_0)+(\omega_m t+\varphi_1-\varphi_0)\} + $$
$$+ a_2 \frac{m}{2} \cos\{(\omega_0 t+\varphi_0)-(\omega_m t-\varphi_2+\varphi_0)\}.$$

This may also be written as:

$$S_u = B_1 \cos(\omega_0 t+\varphi_0) + B_2 \sin(\omega_0 t+\varphi_0) =$$
$$= \sqrt{B_1^2+B_2^2}\cos(\omega_0 t+\varphi_0'), \quad . \quad . \quad . \quad . \quad . \quad (12)$$

where:

$$\left.\begin{aligned} B_1 &= a_0 + a_1\frac{m}{2}\cos(\omega_m t+\varphi_1-\varphi_0) + a_2\frac{m}{2}\cos(\omega_m t-\varphi_2+\varphi_0) \\ B_2 &= \qquad a_1\frac{m}{2}\sin(\omega_m t+\varphi_1-\varphi_0) - a_2\frac{m}{2}\sin(\omega_m t-\varphi_2+\varphi_0) \end{aligned}\right\} (13)$$

It will be seen from (12) that S_u represents a carrier wave of angular frequency ω_0 and of amplitude $\sqrt{B_1^2+B_2^2}$. Since the signal is to be detected in an A.M. detector, the amplitude is all that concerns us.

Applying (13) we find:

$$B_1^2 + B_2^2 = a_0^2 + \frac{a_1^2 m^2}{4} + \frac{a_2^2 m^2}{4} +$$
$$+ a_0 a_1 m \cos(\omega_m t+\varphi_1-\varphi_0) + a_0 a_2 m \cos(\omega_m t-\varphi_2+\varphi_0) +$$
$$+ \frac{a_1 a_2 m^2}{2}\cos(2\omega_m t+\varphi_1-\varphi_2). \quad . \quad . \quad . \quad . \quad (14)$$

Omitting, for the moment, the factor $a_0 m$ common to the fourth and fifth terms, the following expression may be used for the sum of the two:

$$a_1 \cos(\omega_m t+\varphi_1-\varphi_0)+a_2\cos(\omega_m t-\varphi_2+\varphi_0)=$$
$$\left\{a_1\cos(\varphi_1-\varphi_0)+a_2\cos(\varphi_2-\varphi_0)\right\}\cos\omega_m t-$$
$$\left\{a_1\sin(\varphi_1-\varphi_0)-a_2\sin(\varphi_2-\varphi_0)\right\}\sin\omega_m t=$$
$$C\cos(\omega_m t+\psi),$$

where C is a constant, and

$$\tan\psi=\frac{a_1\sin(\varphi_1-\varphi_0)-a_2\sin(\varphi_2-\varphi_0)}{a_1\cos(\varphi_1-\varphi_0)+a_2\cos(\varphi_2-\varphi_0)}.$$

This is formula (4).

If $m \ll 1$, the last term in (14) may be omitted; the amplitude of S_u then corresponds to:

$$\sqrt{B_1^2+B_2^2}=\sqrt{a_0+\left(\frac{a_1 m}{2}\right)^2+\left(\frac{a_2 m}{2}\right)^2+C\cos(\omega_m t+\psi)}.$$

This periodic function can be expanded as a Fourier series containing only cosine functions, viz.:

$$\sqrt{B_1^2+B_2^2}=b_0+\sum_{n=1}^{\infty}b_n\cos n(\omega_m t+\psi).$$

The fundamental term is $b_1\cos(\omega_m t+\psi)$, the phase displacement of which with respect to the modulation of the input signal S_i is ψ (see equation 2). From this the modulation phase delay equation (5) can be derived.

Summary. Phase distortion takes place in a network if the time taken by a signal to travel through the network depends on the frequency of the signal. The time, or rather the delay involved may be either "normal", or "modulation phase delay", depending on whether the signal passes through the network direct, or as modulation on a carrier wave.

The normal phase delay can be derived direct from the phase characteristic of the network, but to determine the modulation phase delay the amplitude characteristic is also required. In practice the best method of establishing the phase characteristic is to determine its *derivative* as a function of the frequency, which, ignoring the sign, is designated the "group delay".

An instrument with which group delay in networks, and more especially in television receivers, can be measured accurately to within 10^{-9} sec. is described in this article. Group delay is determined by measuring phase differences; hence the instrument is really a very sensitive phase difference meter operating on the principle that the phase shift to be measured affects the frequency of an oscillatory circuit when introduced into the latter. A discriminator is used to convert the change in oscillation frequency thus produced into a voltage variation, which is then measured with a valve voltmeter calibrated in nanoseconds (10^{-9} sec) enabling direct reading of the group delay or in most cases a difference in group delay.

Measurements on the video stage of a television receiver, involve certain complications which necessitate the use of a special adaptor. The results of some practical measurements are included in this article as an example of the kind of information obtainable by means of the instrument.

THE SPECIFIC LIGHT OUTPUT OF "PHOTOFLUX" FLASH-BULBS

by L. H. VERBEEK.

771.448.4

The very small and inexpensive flash bulb, type PF 3, which was marketed in 1952, has been enthusiastically received by photographers of all countries. This article outlines the developments which have led to the manufacture of this bulb and of the similar, larger types (PF 14 and PF 25).

The open flashlight with magnesium powder in common use for indoor snapshots a quarter of a century ago, has now been almost entirely superseded by the well-known glass-enclosed flash-bulb.

The advantages of this lamp are many — it is more reliable than the open flashlight powder, there is no risk of fire, it has a shorter flash duration, and, finally, it made it possible to synchronize the flash with the opening and closing of the shutter — an essential feature of modern flash photography.

All these advantages, however, would not have ensured the present popularity of the flash-bulb, if it had not met one essential requirement, viz. to give a satisfactory light output at a reasonable price.

This implies that the bulb should not be too large, or in other words, that the specific light output of the bulb, i.e. the light output per unit volume should be sufficiently high. (The light output is defined as the number of "visual" lumen-seconds obtained from integration of the total area of the light-time characteristic, or "flash curve", *fig. 1*).

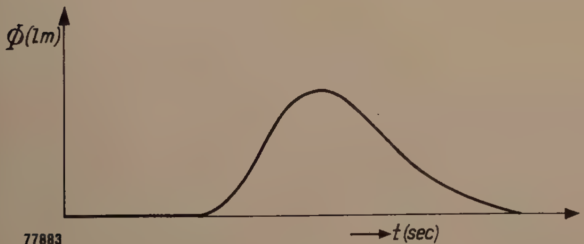

Fig. 1. Luminous flux Φ in visual lumens, emitted by a flash-bulb, plotted as a function of time [1]) (schematically). By integration over this "flash curve", the total emitted light in "visual" lumen-seconds is obtained. (For "visual" and "photographic" lumen-seconds, see the article referred to in [3]).)

Since the first introduction of "Photoflux" lamps by Philips, their development has been largely characterized by a constant striving after the greatest possible specific light output. The demands as regards total light output have not risen during the last twenty-five years; rather they have decreased owing to the use of faster lenses and more sensitive photographic emulsions. The demand for the smallest possible volume (and thus low price) for a given light-output, however, has become steadily more and more pressing. This has been partly due to competition between the various flash-bulb manufacturers, and partly also to the growing popularity of this source of lighting: the more flash-bulbs one wants to use, the more essential are both a low price and a small size. For the press photographer, the success of his work often depends upon the number of flash-bulbs he can carry in his pockets.

These demands have been answered by the impressive rise in the specific light output of the "Photoflux" bulbs since their introduction in 1932. This is shown in *fig. 2*. A certain reserve is necessary with respect to the earlier measurements (before 1945) incorporated in this graph, since at that time the measuring technique had not yet been standardized. Even if the error in the pre-1945 measurements is estimated to be as high as 20%, however, the enormous rise in the specific light output illustrated by fig. 2, is not invalidated.

The various jumps in this line of development correspond to certain alterations in the construction, or in the manufacturing methods of the "Photoflux" bulbs. The last great jump, made about a year and a half ago, corresponds to the marketing of the PF 3, which is the smallest flash-bulb ever made *). In this article a short description will be given of the modification in flash-bulb manufacture which made this last jump possible. As an introduction to this, it is desirable to consider in some detail, the steps in the development of flash-bulb design, corresponding to the previous jumps depicted in the graph.

In the very first "Photoflux" bulbs, the light was produced by the explosive reaction of two gases, approximately 30% by volume of carbon disul-

[1]) A method for recording such flash curves has been described by J. A. M. van Liempt and J. A. de Vriend, Rec. Trav. chim. Pays-Bas 52, 160, 1933. For the measuring method standardized at present, see Am. Federal Specification WL 122.

*) Note added in proof: The development in America of a still smaller flashbulb has recently been announced.

phide vapour (CS_2) and approximately 70% of nitrogen monoxide, (NO), contained as a mixture in the bulb.

In 1934 an entirely new principle was introduced. Now the light was produced by the combustion of a quantity of very fine wire (only 32 microns thick) of an aluminium-magnesium alloy [2]). The bulb was filled with a loosely knit ball of this wire, together with an ample amount of oxygen. The volume was chosen so as to obtain a relatively low pressure (25 cm Hg), in order to prevent the bulb exploding upon ignition.

A different technique, developed earlier by others, and likewise producing satisfactory results, was based upon the combustion of very thin aluminium foil in oxygen. Filling the bulbs with wire instead of with foil made possible a higher degree of mechanization of the production process, so that the bulb could be made more cheaply. Also, the fact that the flash curve of a wire-filled bulb is broader than that of a foil-filled bulb (*fig. 3*), was later found to be a considerable advantage, as this permitted easier and more reliable synchronization [3]). Finally, with respect to the specific light output, the wire-filled bulb is to be preferred to the foil-filled bulb, since with a tangle of wire, the light produced in the initial stage of the combustion is absorbed to a far less degree by the yet unburnt metal than in the case of foil; thus with the same volume, more light is produced. The less steep flash curve, moreover, is associated with a lower peak-value of the pressure during combustion; consequently, a wire-filled bulb can be filled to a higher oxygen-pressure, so that a smaller bulb volume suffices for the same light output and for the same safety-margin against explosion.

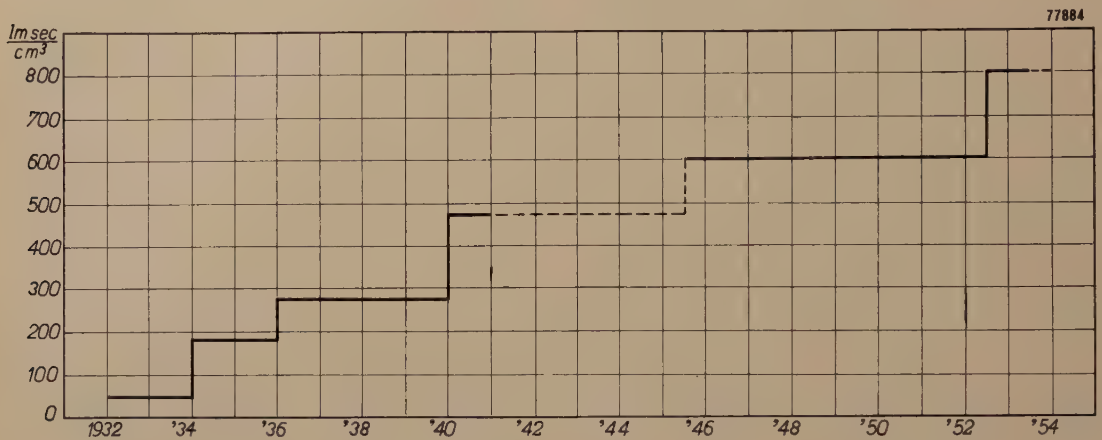

Fig. 2. The specific light output (number of visual lumen-seconds divided by the bulb volume) of "Photoflux" bulbs over the course of the years. For each year, the type with the greatest specific light output of the bulbs then available is represented.

Considerations of the last-mentioned design detail are also the basis of the next step forward shown in the graph of fig. 2. It was realized that with a wire-ball, since all metal parts are easily accessible to the oxygen, it was unnecessary to have *excess* oxygen available for combustion. If *chemically equivalent* quantities of metal and oxygen are used, no superfluous gas is present to be heated to high temperatures during combustion. This means lower peak pressures, and consequently the bulb can be filled with oxygen to a higher initial pressure. Hence the required amount of oxygen can be enclosed in a

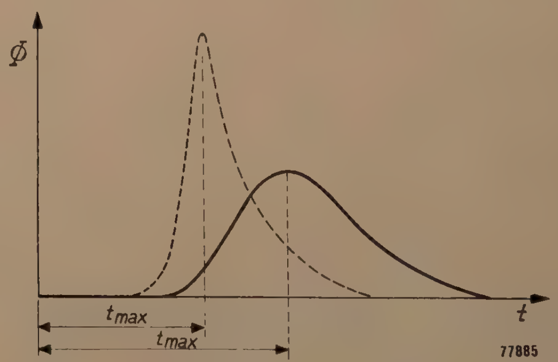

Fig. 3. Flash curves (schematic) of a bulb filled with Al-Mg wire (full curve), and of one filled with Al-foil (dotted curve). The foil-filled bulb has a higher, but narrower peak than the wire-filled bulb. Also the time to peak i.e. the period t_{max} from the moment of ignition till the reaching of the maximum luminous flux, is, as a rule, considerably shorter for the foil-filled lamp.

2) See J. A. M. van Liempt and J. A. de Vriend, Philips tech. Rev. **1**, 289-294, 1936.

3) G. D. Rieck and L. H. Verbeek, Philips tech. Rev. **12**, 185-192, 1951.

smaller bulb (the volume of the wire is very small in comparison to that of the oxygen and may, therefore, be neglected).

The further steps in the graph, those representing the years 1940 and 1946, are due to the introduction of a tough, protective layer of lacquer, first applied on the inside, and later also on the outside of the bulb. The reduction of the explosion risk thus obtained, permitted the use of even higher oxygen pressures. This development has already been extensively dealt with in this Review [3]).

Further research into the conditions under which explosion of a glass bulb occurs, revealed that, in order to withstand high pressures, the wall need not necessarily be very thick, provided that it is of very uniform thickness in the region of the largest diameter of the bulb, and that the latter is strictly rotationally symmetrical.

This work introduced the possibility of using bulbs made, instead of by blowing directly from the molten mass, from high-speed drawn machine-made glass tubing, which is given the required shape by locally heating and blowing in a mould. For not too large bulbs, this process can be so conducted that a very uniform wall thickness can indeed be obtained. The small bulbs for torch lamps, for example, are manufactured in this way. Although the wall thickness of these bulbs at their largest diameter amounts to barely 0.3 mm, it has been found from regular checks that on the average they can withstand static pressures of between 15 and 20 atmospheres. On the other hand, the above-mentioned investigation revealed that in the types of "Photoflux" bulbs manufactured since 1946, the peak pressures during ignition did not exceed a value of approximately 4 atmospheres. There remains, it is true (and this applies to bulbs of every shape), a certain risk that during ignition the bulb may be weakened by hot particles of ash, which may cause cracks in the glass (see the article referred to in [3])). The risk of explosion due to this cause is obviated by the tough coating of lacquer applied to the outside of the bulb. The lacquer coating itself is capable of withstanding a pressure of 3 to 5 atmospheres!

These results led to a manufacturing technique similar to that of small incandescent lamps such as torch bulbs. This method of manufacture allows the bulb volume to be used to its fullest extent as will be seen presently.

In this way, and also by using a higher filling pressure, a specific light output of about 700 lm sec/cm³ has been obtained for the PF 3 flash-bulb; for the later, slightly larger types PF 14 and PF 25, this value has been raised to 800 lm sec/cm³.

The most recent jump in the graph of fig. 2 corresponds to the introduction of this new manufacturing technique; cf. *table I.*

Table I. Data regarding the new "Photoflux" bulbs

Type	Bulb diameter (mm)	Quantity of Al-Mg wire (mg)	Light output (lm sec)	Bulb volume (cm³)	Spec. light output (lm sec/cm³)
PF 3	22	11	5 500	8	700
PF 14	26.5	22	11 000	14	780
PF 25	30	34	16 000	20	800

The greater specific light output is not the sole reason for the lower price of the new bulbs compared with equivalent earlier types. The present method of manufacture, because it is particularly suited to large-scale mass production, was also an important factor in lowering the prices (high-speed machines, less glass scrap).

Figs 4 and *5* show the method of construction of the "Photoflux" bulbs in the old and the new manufacturing processes respectively. In the old, conventional process, construction starts from the

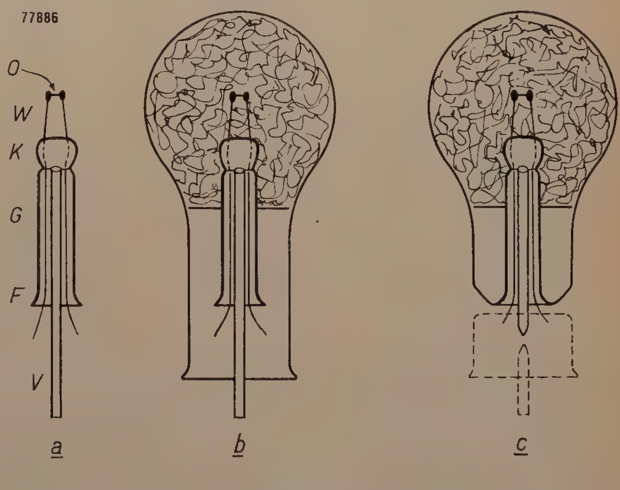

Fig. 4. Construction of a "Photoflux" bulb by the old process. The "pinch" (*a*) consists of a piece of glass tubing *G*, pinched (at *K*) around the two lead-in wires *W* carrying the igniting filament *O*, and is provided with an exhaust tube *V*. After the pinch has been placed inside the bulb (*b*), its flange *F* is fused to the neck of the bulb (*c*).

well-known "pinch mount". This consists of a piece of glass tubing pinched at one end round the two lead-in wires, and flanged at the other end; an exhaust tube is also fused in the pinch. The ignition filament is mounted between the two lead-in wires, and is coated with a primer paste, which on heating, fires the curled wire. The bulb is filled with the

curled wire, the pinch is placed inside and the flange is then fused to the neck of the bulb. The bulb is evacuated and filled with oxygen via the exhaust tube. After sealing-in, a considerable part of the neck of the bulb and of the exhaust tube is lost as scrap glass. After pumping, a cap is cemented to the bulb.

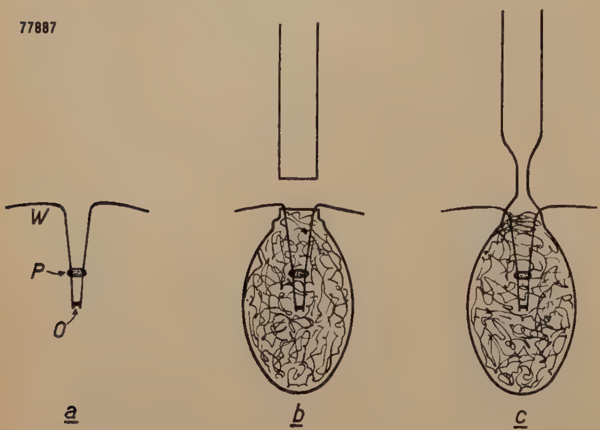

Fig. 5. Manufacture of the new "Photoflux" bulbs, with a "bead mount". The bead mount (*a*) simply consists of the two lead-in wires *W* carrying the filament *O*, fused into a glass bead *P*. This mount it suspended in the bulb (*b*), which has been blown from thin glass tubing. By fusing to this a piece of the same glass tubing (*c*), the lead-in wires are sealed-in, and the bulb is provided with an exhaust tube (which itself, after sealing off, provides the material for blowing the next bulb).

The new process (fig. 5), starts from a far simpler and smaller "mount", consisting solely of the two lead-in wires, fused into a glass bead. The ignition filament, coated with the primer paste, is mounted between the two wires as before. This "bead mount", as it is called, is suspended in the wire-filled bulb, the latter having been blown from glass tubing in the manner described above. After this, an exhaust tube of the same glass tubing is fused to the neck of the bulb. The two lead-in wires are sealed-in by the same operation. After pumping, filling with oxygen and sealing-off the tube, another bulb can be blown from the remainder of the exhaust tube, so that hardly any glass is wasted.

The PF 14 which is now being manufactured according to this technique, has a light output of approx. 11 000 lm sec, i.e. the same output as was obtained from the first "Photoflux" bulbs, marketed in 1932. The volume of the PF 14, however, is only about 1/20 of that of the old bulb. *Fig. 6* gives a graphic impression of the overall increase in specific light output since 1932 as depicted in fig. 2.

A few words should be said about the differences in the specific light output of the three bulbs of the new type (see table I). The bulb volumes are proportional to the quantities of the curled wire,

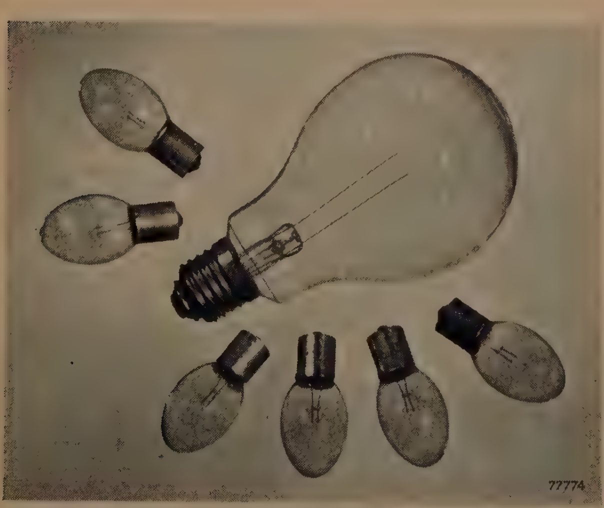

Fig. 6. A "Photoflux" bulb of 1932 with carbon-disulphide filling, compared with some flash bulbs of the modern type PF 14, which gives the same light output.

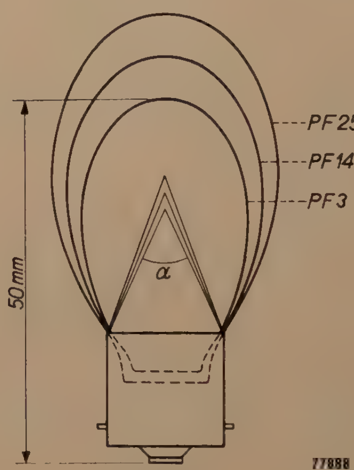

Fig. 7. The three flash bulbs PF 3, PF 14 and PF 25 have identical caps, but the bulbs are, of course, of different sizes. The angle α subtended by the cap at the centre of the bulb, is a measure of the screening effect of the cap.

since for each case equivalent quantities of oxygen are used, and the filling pressure is the same in each case. One would thus expect, provided that the light output per milligram of metal (the "efficiency") remains the same, an equal value of the specific light output for the three types. On further investigation, in fact, it has been found that the differences in the measured specific light output are *not* due to differences in efficiency, but to light losses caused by the firing paste and by the bulb cap. The three lamp types of table I have identical caps. With the smallest bulb this screens off a substantially greater portion of the light than is the case with the largest; see *fig.* 7. The firing paste, furthermore, causes a loss of light (presumably through smoke development), the percentage of which is not the same for all types; moreover, it is necessary to use firing pastes

of a different composition in order to obtain an equal ignition time (time to peak, see fig. 3) for all bulb types.

Table II shows the above-mentioned light losses for the three bulb types of table I, together with the gross specific light output obtained by adding these losses to the measured specifiic light output. From this it can be seen that the gross specific light output is practically the same for all types.

Table II. Light losses with different types of "Photoflux" bulbs

Type	Screening angle of the bulb cap	Light loss due to bulb cap %	Light loss due to ignition paste %	Gross specific light output (lm sec/cm³)
PF 3	55°	18	15	940
PF 14	45°	14	7.5	960
PF 25	40°	12.5	5	945

Summary. The light output of a flash-bulb per unit volume of the bulb is a very important factor, both with respect to the costs and to ease of handling. A graph shows how this specific light output has enormously increased since the introduction of the first "Photoflux" bulbs (1932). The article reviews the various constructional alterations in "Photoflux" bulbs which have contributed to this rise. The latest step forward has been made with the introduction of the PF 3, the smallest flash bulb in the world. By the use of a manufacturing technique similar to that used for torch bulbs, employing a bead mount, this flash-bulb has been kept very small and also low in price. The PF 14 and PF 25, at present manufactured by the same technique, have a specific light output of 800 lm sec/cm³, i.e. a value 20 times as large as that of the first "Photoflux" bulbs.

ABSTRACTS OF RECENT SCIENTIFIC PUBLICATIONS OF N.V. PHILIPS' GLOEILAMPENFABRIEKEN

Reprints of these papers not marked with an asterisk * can be obtained free of charge upon application to the administration of the Philips Research Laboratory, Eindhoven, Netherlands.

2045: F. A. Kröger and J. A. M. Dikhoff: The function of oxygen in zinc sulphide phosphors (J. Electrochem. Soc. **99**, 144-154, 1952, No. 4).

At 1200 °C ZnS and ZnO form solid solutions: ZnS dissolves 1 mole per cent ZnO, while ZnO forms a solution with 0.3 mole per cent ZnS. The incorporation of ZnO in ZnS causes the appearance of a new absorption band and, in the presence of activators, of new fluorescence bands displaced about 150 Å toward longer wavelengths with respect to the original bands. These effects are explained by the assumption of separate oxygen levels 0.1 eV above the filled band and of new centres consisting of associated pairs of oxygen and activator ions. The formation of such pairs is explained on the basis of the principle of compensation of volume. This principle also explains the favourable effect of oxygen on the intensity of fluorescence. It is found to be the logical complement of the principle of compensation of charge, introduced earlier in connection with the incorporation of ions of a certain valency in a base lattice consisting of ions of a different valency. It is shown that oxygen gives rise to characteristic traps and has further a marked effect in combination with fluxes. The optical properties of ZnO-x(ZnS) are briefly described and explained along similar lines.

2046: J. I. de Jong and J. de Jonge: The reaction of urea with formaldehyde (Rec. Trav. chim. Pays-Bas 71, 643-660, 1952, No. 6).

The reaction of urea and formaldehyde, giving monomethylolurea, is reversible in a neutral, acid or alkaline aqueous solution, the forward reaction being bimolecular and the reverse reaction monomolecular. The forward and reverse reactions are catalyzed to the same extent by hydrogen ions as well as by hydroxyl ions. The specific rates are directly proporional to the hydrogen ion and hydroxyl ion concentrations. There appears to be an influence of the buffer concentration on the reaction rates, probably due to a general acid and general base catalysis. The equilibrium is almost independent of the *pH* of the solution and of the buffer concentrations. The activation energies of the forward and the reverse reaction have been determined, giving the heat of reaction. Within experimental error, these activation energies may be the same for the non-catalyzed and for the catalyzed system. The reaction mechanism is discussed.

2047: J. I. de Jong and J. de Jonge: The formation and decomposition of dimethylol urea (Rec. Trav. chim. Pays-Bas 71, 661-667, 1952).

The formation and decomposition of dimethylol urea shows a close resemblance to that of mono-

methylolurea previously studied (see Abstract No. 2046). The reaction between formaldehyde and monomethylolurea giving dimethylolurea leads to an equilibrium which can be reached from both sides. The equilibrium is independent of the *pH* of the solution. The formation of dimethylolurea from formaldehyde and monomethylolurea appears to be a bimolecular reaction. The decomposition of dimethylolurea is monomolecular. Both reactions are catalyzed to the same extent by hydrogen ions and by hydroxyl ions and there is an influence of the buffer concentration on the velocity. The reaction rates are found to be directly proportional to the hydrogen ion and hydroxyl-ion concentrations. The activation energies have been determined. Within experimental error, these energies are found to be about the same as the activation energies of the monomethylolurea formation and decomposition, viz. 14 and 19 kcal/mole. The reaction mechanism is briefly discussed.

2048: K. F. Niessen: Spontaneous magnetization of nickel zinc ferrite as a function of the nickel zinc ratio (Physica **18**, 449-468, 1952, No. 6-7).

The reduced spontaneous magnetization I_f^* of nickel zinc ferrite (magnetization at temperature T, divided by that at absolute zero) is determined as a function of the reduced temperature T^* (T, divided by the Curie temperature T_c) and of the nickel-zinc ratio f. The latter is defined by the following expression for the ratio between the numbers of nickel and zinc ions: $\mathrm{Ni/Zn} = f/(1-f)$. In the case $T^* \ll 1$ and in the case $T^* = 1 - \Delta$ $(\Delta \ll 1)$ formulae for the reduced magnetization are given, holding for high values of f, e.g. for $1/2 < f < 1$. For intermediate values of T^*, a graphical method must be used. The results are compared with the experimental curves of Guillaud and Roux, which give the reduced magnetization as a function of T^* of several ferrites with various nickel-zinc ratios, especially at low and intermediate values of T^*. The curves diverge in a typical way. This can be explained qualitatively.

2049: H. Bremmer: On the asymptotic evaluation of diffraction integrals with a special view to the theory of defocusing and optical contrast (Physica **18**, 469-485, 1952, No. 6-7).

An expansion is given of the function $u(x, y, z)$ that satisfies the scalar wave equation in the half-space $z < 0$ and is equal to a given distribution u_0 (x, y) in the plane $z = 0$. If u_0 is zero beyond a closed contour L in $z = 0$, $u(x, y, z)$ splits into a so-called geometrical-optical part (which vanishes outside the cylinder passing through L and having generating lines parallel to the z-axis) and a diffraction part (determined by the values of u_0 near L). Each part can be expanded into terms depending on $u_0(x, y)$ itself and on its iterative two-dimensional Laplace operators $\Delta^n u_0 = (\partial^2/\partial x^2 + \partial^2/\partial y^2)^n\ u_0\ (x, y)$. The expansions are in general asymptotic for small wavelengths; however, their exact validity can be proved for functions u_0 that are polynomials inside the contour L. The terms of the diffraction part consist of contour integrals along L, the corresponding terms for the geometrical-optical part do not depend on any integration. The first few terms of the latter part are essential for defocusing effects and can be connected with the brightness contrast existing in the plane $z = 0$.

2050: G. Diemer, Z. van Gelder and J. J. P. Valeton: Interference in television pictures (Wireless Engineer **29**, 164-168, 1952, No. 345).

Interference in the form of vertical lines on the left-hand side of a television picture has been studied. It can be attributed to intrinsic properties of the I_a-V_a characteristics of the power valve used for generating the line-deflection current. These properties cause irregularities in the anode current and give rise to signals of very high frequency, which may penetrate into the r.f. or i.f. amplifier of the receiver.

2051*: J. J. Went, G. W. Rathenau, E. W. Gorter and G. W. van Oosterhout: Hexagonal iron-oxide compounds as permanent-magnet materials (Phys. Rev. **86**, 424-425, 1952, No. 3).

A short survey of the comprehensive article in Philips tech. Rev. **13**, 194-208, 1952, No. 7.

2052*: J. S. C. Wessels and E. Havinga: The redox potential as a critical factor in the Hill reaction (Rec. Trav. chim. Pays-Bas **71**, 809-812; 1952, No. 7).

The photochemical reduction of various quinones and dyes by water, in the presence of chloroplasts, was studied by measurement of the redox potential during illumination. Whether this so-called Hill reaction will proceed to a measurable degree, appears to be determined by the standard potential of the redox substance. With systems having a standard redox potential of about 40 millivolts or lower, no reduction was observed.

2053: J. de Jonge, R. Dijkstra and G. L. Wiggerink: The quantum yield of the photo-decomposition of some aromatic diazonium salts (Rec. Trav. chim. Pays-Bas 71, 846-852, 1952, No. 8).

The quantum yield of the photo-decomposition of some aromatic diazonium salts in solution is estimated, using light with a wavelength of 3560 Å. The photo-decomposition of phenyl-amino benzene diazonium sulphate is proposed as a suitable actinometer. The quantum yield of the photochemical isomerisation of the stable form of p-methoxybenzene diazo-cyanide was found to be about 0.35.

2054: J. I. de Jong and J. de Jonge: The reaction between urea and formaldehyde in concentrated solutions (Rec. Trav. chim. Pays-Bas 71, 890-898, 1952, No. 8).

The nature and the velocities of the reactions occurring in concentrated solutions of urea and formaldehyde are very similar to those found in dilute systems. A rapid initial reaction between urea and formaldehyde, as reported in literature, was not observed, and is shown to be due to the analytical methods used.

2055: K. H. Klaassens and C. J. Schoot: The preparation of 1-methyl-2-hydroxy-3-diazobenzene-5-sulphonic acid (Rec. Trav. chim. Pays-Bas 71, 920-924, 1952, No. 8).

The presentation of 1-methyl-2-hydroxy-3-diazobenzene-5-sulphonic acid, starting from o-cresol, is described. With a small quantity of a strong acid a suspension of 1-methyl-2-hydroxy-3-aminobenzene-5-sulphonic acid in a solution of sodium nitrite gives the sodium salt of the diazonium compound.

2056: J. G. Bos, R. J. H. Alink and C. J. Dippel: Photodecomposition of aqueous solutions of diazonium salts in the presence of mercurous ions. (Rec. Trav. chim. Pays-Bas, 71, 945-953, 1952, No. 8).

Photodecomposition of aqueous solutions of o-hydroxydiazonium salts leads to the formation of mercury with a disproportion of mercurous ions, in contrast to p-aminobenzene diazonium salts, where mercury only results from reduction of mercurous ions by the photodecomposition products.

2057: H. Bremmer: The derivation of paraxial constants of electron lenses from an integral equation (Appl. sci. Res. **18**, 416-428, 1952, No. 6).

The paraxial trajectories in electron lenses are derived from an integral equation. The Liouville-Neumann expansions of the solutions of this equation lead to expressions for the magnification, the focal distances and the positions of the focal points and cardinal points. The number of integrations to be performed in the individual terms of the expansions is halved, as compared with the normal treatment. The focal and cardinal points are defined as osculating elements similar to those introduced by Glaser.

2058: A. H. Boerdijk: A new aspect in the calculation of toothed gearing (Ingenieur **64**, W63-W65, 1952, No. 37).

This paper deals with the calculation of the numbers of teeth of the wheels in a gearing with a prescribed gear ratio, equal to the quotient of two integers k/l. The known methods of decomposing k and l into prime factors and of developing k/l in continued fractions often fail to give a practical and exact solution. A new method is described, based on the introduction of planet gearings (or simple differentials) in the conventional gearing. Practical and exact solutions can be obtained for arbitrary values of k and l, even for very large primes.

2059: G. W. Rathenau, J. Smit and A. L. Stuyts: Ferromagnetic properties of hexagonal iron-oxide compounds with and without a preferred orientation (Z. Phys. **133**, 250-260, 1952, No. 1-2).

The article deals with the magnetisation of hexagonal iron-oxide compounds as a function of the magnetic field strength. It is shown that crystal imperfections must play a role in the formation of Bloch-Walls. In the case of random orientation of the crystallites, and with crystallites of dimensions greater than a certain critical value, demagnetization by displacement of Bloch-Walls already occurs at positive field-strengths $H \approx 4\pi I_s$ ($\mu_0 H \approx J_s$). By preparing specimens with oriented crystals, BH-values as large as 3×10^6 gauss. oersted ($BH \approx 2.5\ 10^4$ J/m^3) are obtained. Crystal growth causes an increase in the preferred orientation. An explanation of this effect is given. (See also Philips tech. Rev. **14**, 194-208, 1952, No. 7).

2060: J. Smit: The influence of elastic shear strains on the conductivity and thermo-electric force of cubic metals (Physica **18**, 587-596, 1952, No. 8/9).

Elastic shear strains cause a change in the shape of the Fermi surface of metals. The influence that such a change has upon the electrical conductivity

and the thermo e.m.f. has been calculated for monovalent face-centered cubic metals, and the results have been compared with the experimental values for Cu, Ag and Au. The theory also accounts qualitatively for the experimental values of trivalent Al.

2061: P. M. van Alphen, C. G. E. Burger, W. J. Oosterkamp, M. C. Teves and T. Tol: Detailerkennbarkeit bei Durchleuchtung und Photographie mit der Bildverstärkerröhre (Fortschr. Röntgenstrahlen-Röntgenpraxis 77, 469-470, 1952, No. 4). (Performance of an X-ray image intensifier with visual and photographic observation; in German).

A "Bakelite" thorax phantom was used to test the performance of an X-ray image intensifier. The visual acuity during fluoroscopy in a room with fair illumination after 1 minute of adaptation and with only 1/5 of the dose rate is almost twice as good as during ordinary fluoroscopy. Photographs of the intensified image can be made with 1/10 of the energy used for ordinary contact photographs and 1/50 of the energy used for ordinary camera photographs. These photographs show a resolution of detail which lies midway between contact photography and ordinary fluoroscopy. The results are in good agreement with calculated data based upon the photon-fluctuation theory of Morgan and Sturm.

2062*: G. W. Rathenau: Grain growth observed by electron-optical means (L'état solide, Rapp. 9 Cons. Phys., Inst. int. Phys. Solvay, 25-29 Sept. 1951, Stoops, Brussels 1952, p. 55-72).

Observation of grain growth in cold rolled homogeneous Ni-Fe alloys on annealing (see abstracts **1986** and **2026**). The grain growth which accompanies the α-γ phase transformation of a Si-Fe alloy has also been studied by electron-optical means. Since, in equilibrium, the Si-content of the α phase surpasses that of the γ phase, the velocity of phase boundary movement depends essentially on the concentration gradient which determines the diffusion at the moving boundary. In agreement with expectation, the advancing boundary of a γ grain curve is often heavily convex towards the disappearing α grains. γ grains repel each other because of the high Si content of the α phase in between. The grains of the growing phase are thus enveloped by material having the structure and orientation of the disappearing phase. On lowering the temperature these α inclusions lead to roughly the initial α structure, while on quickly heating they give rise to nuclei of δ phase.

2063: K. H. Klaassens and C. J. Schoot: Preparation of 2-ethoxy-4-diethylaminobenzene-1-diazonium borofluoride (Rec. Trav. chim. Pays-Bas 71, 1086-1088, 1952, No. 9/10).

Description of the preparation of the compound named in the title. A stable diacetyl derivative is formed by treating 2-ethoxy-4-diethylamino-1-aminobenzene with acetic anhydride.

2064: H. B. G. Casimir: Algemene beschouwingen over ruis (T. Ned. Radiogenootschap 17, 199-206, 1952, No. 5/6). (General considerations on noise; in Dutch).

General considerations on noise (thermal and corpuscular) as an introduction to a symposium on this subject.

2065: F. L. Stumpers: De signaal-ruisverhouding bij verschillende modulatiesystemen (T. Ned. Radiogenootschap 17, 249-260, 1952, No. 5-6). (The signal-to-noise ratio for different modulation systems; in Dutch).

A survey is given of the signal-to-noise ratio in the output of different modulation systems as a function of the same ratio in the transmission channel and of the necessary bandwidth. Pulse and carrier wave systems are considered. Attention is drawn to the noise-improvement threshold. It is shown that coded systems, like PCM and delta-modulation, are nearly immune to the noise in the channel, but that in their case the approximative nature of the pulse waveforms themselves introduces quantization noise.

2066: J. de Jonge: Evaporation of mercury from a solution of a mercurous salt at room temperature (Rec. Trav. chim. Pays-Bas 71, 1209-1212, 1952, No. 11).

It is shown that a solution of mercurous nitrate gives off mercury vapour at room temperature, due to the occurrence of the equilibrium

$$Hg^{2+} \rightleftarrows Hg^{2+} + Hg.$$